SMOS Satellite L-band Radiometer: a new Capability for Ocean Surface Remote Sensing in Hurricanes

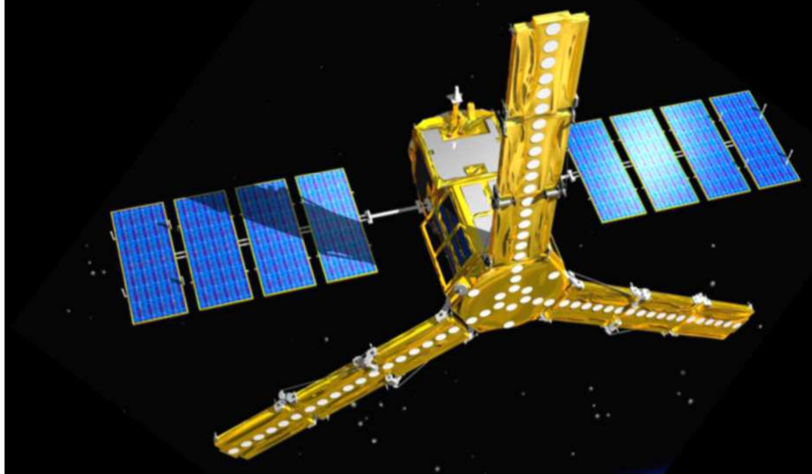

Nicolas Reul[1], J. Tenerelli[2], B.Chapron[1], Y. Quilfen[1], D. Vandemark and Y. Kerr[3]

[1]IFREMER, Laboratoire d'Océanographie Spatiale, Plouzané, France
[2]CLS, Plouzané, France
[3] CESBIO, Toulouse, France

SMOS SCIENCE WORKSHOP
27-29 September 2011 – Arles – France

Outline

- Context
- Review of our understanding of L-band Radiometry at High Winds
- IGOR Hurricane Case Study
- Perspective

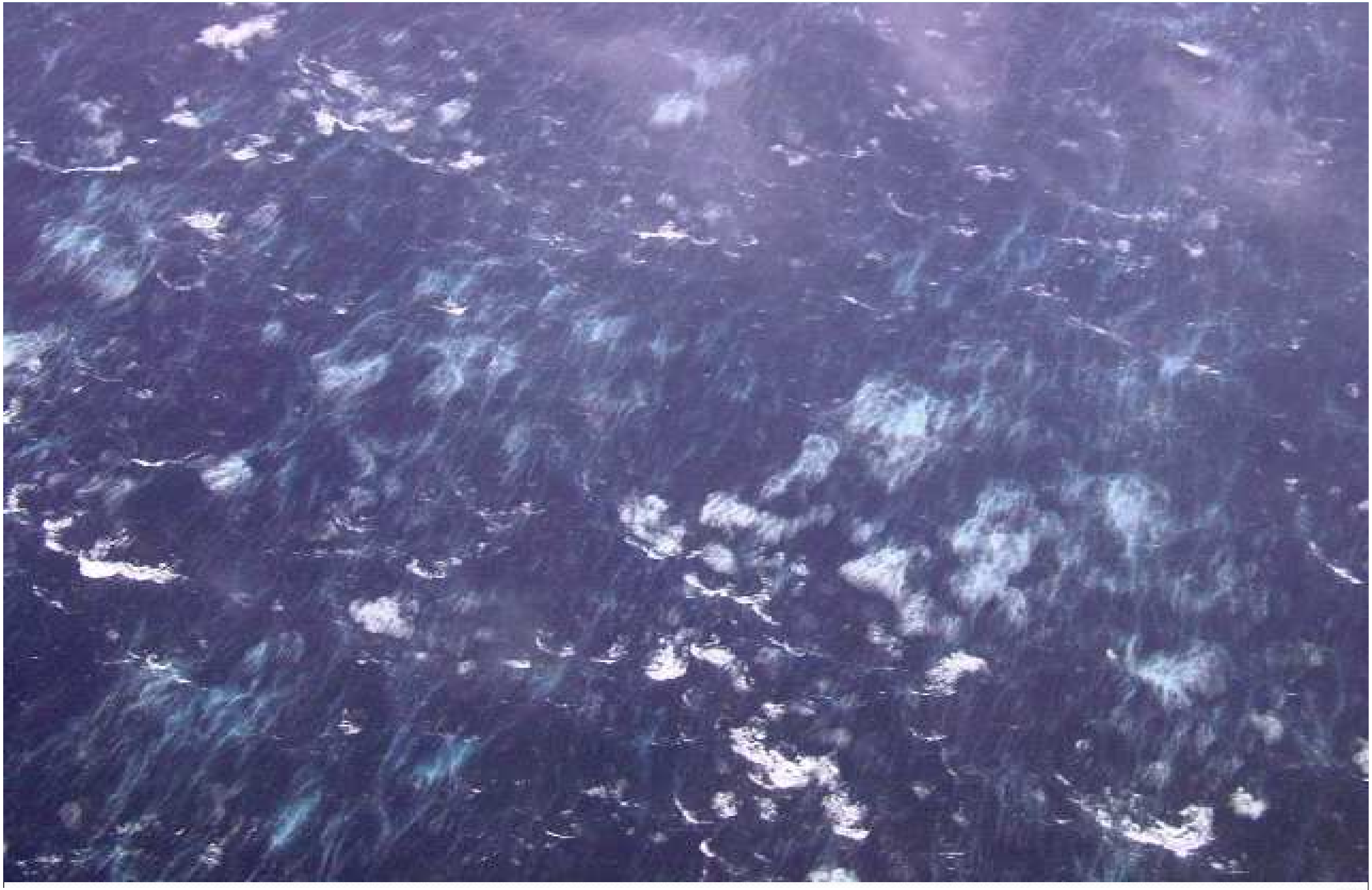

Figure 1: Photograph of the sea surface during a hurricane (Beaufort Force 12) taken from a NOAA ‘‘Hurricane Hunter’’ aircraft (Black *et al.*, 1986).

A complex distribution of two-phase oceanic phenomena

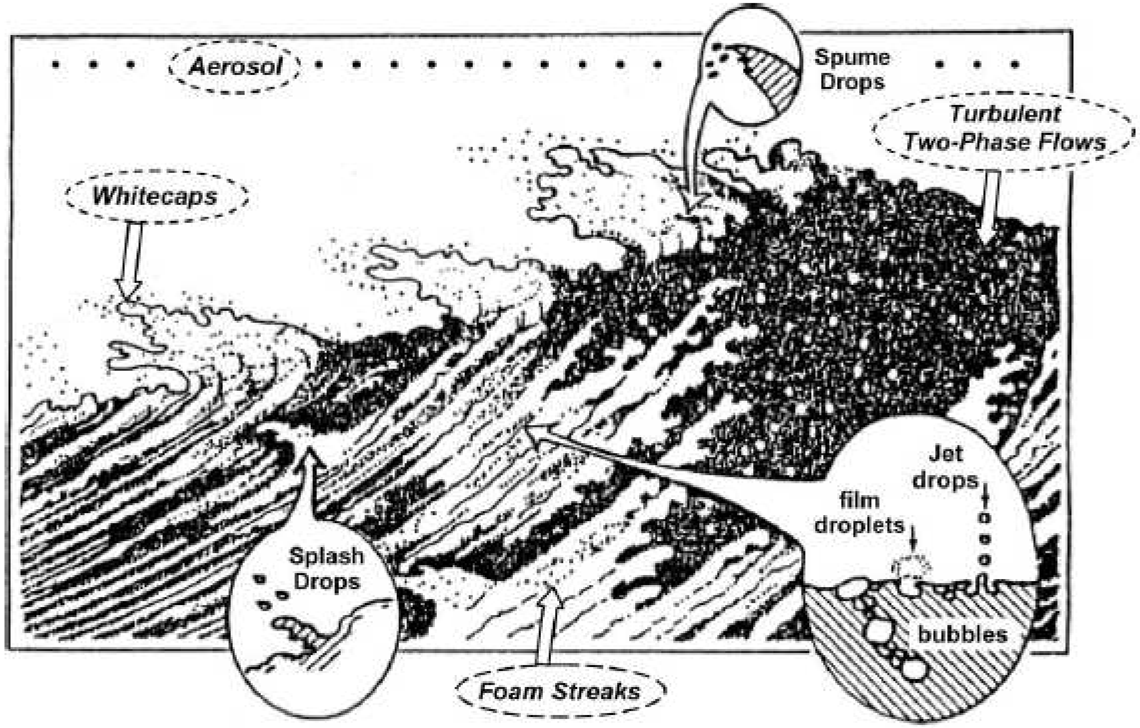

Fig. 1. Classifications of oceanic dispersed media for remote sensing.

Very Complex Sea State distributions

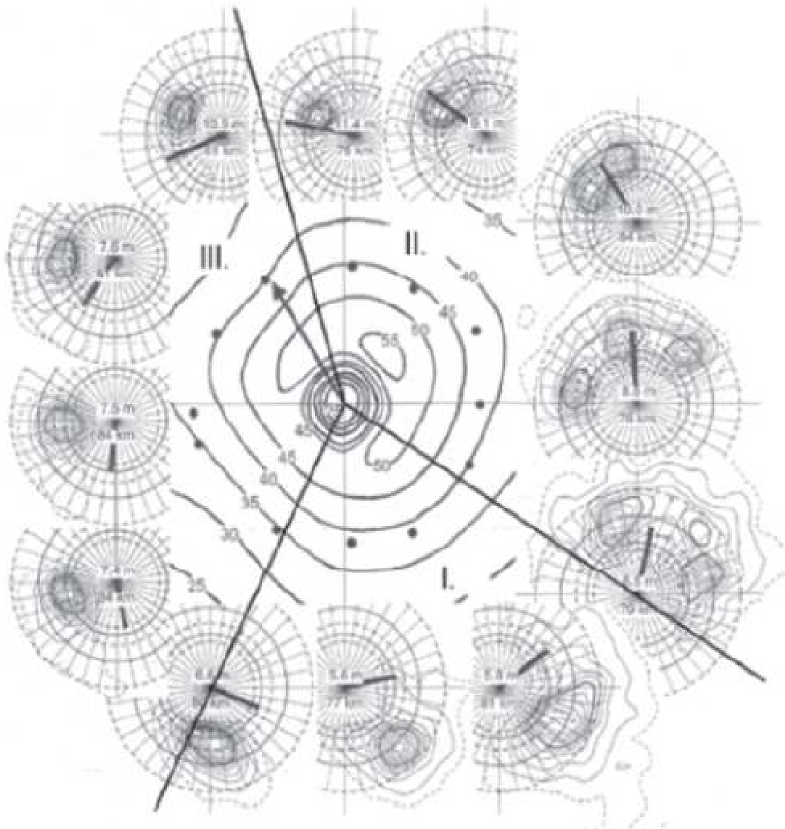

Figure 9: Sea State 2D wave spectra measured by an airborne Scanning Radar Altimeter aroud the eye of hurricane Yvan (2004). Contours of the wind field structure from H*WIND analysis are provided as well (Black et al., 2007)

Significant wave-height

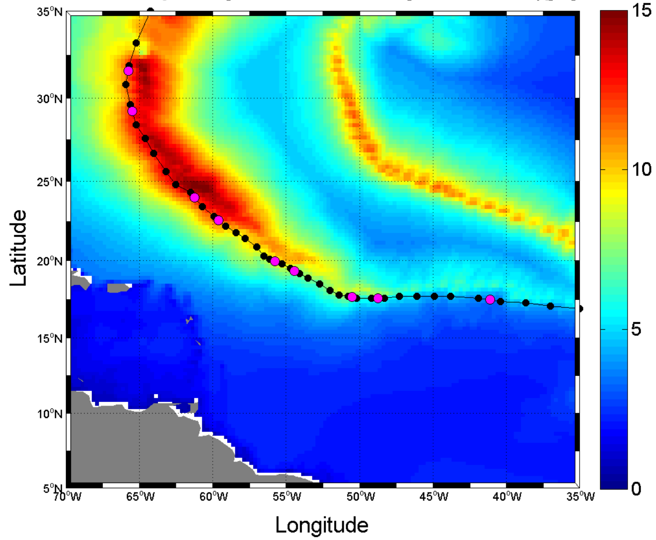

Extreme Sea State conditions

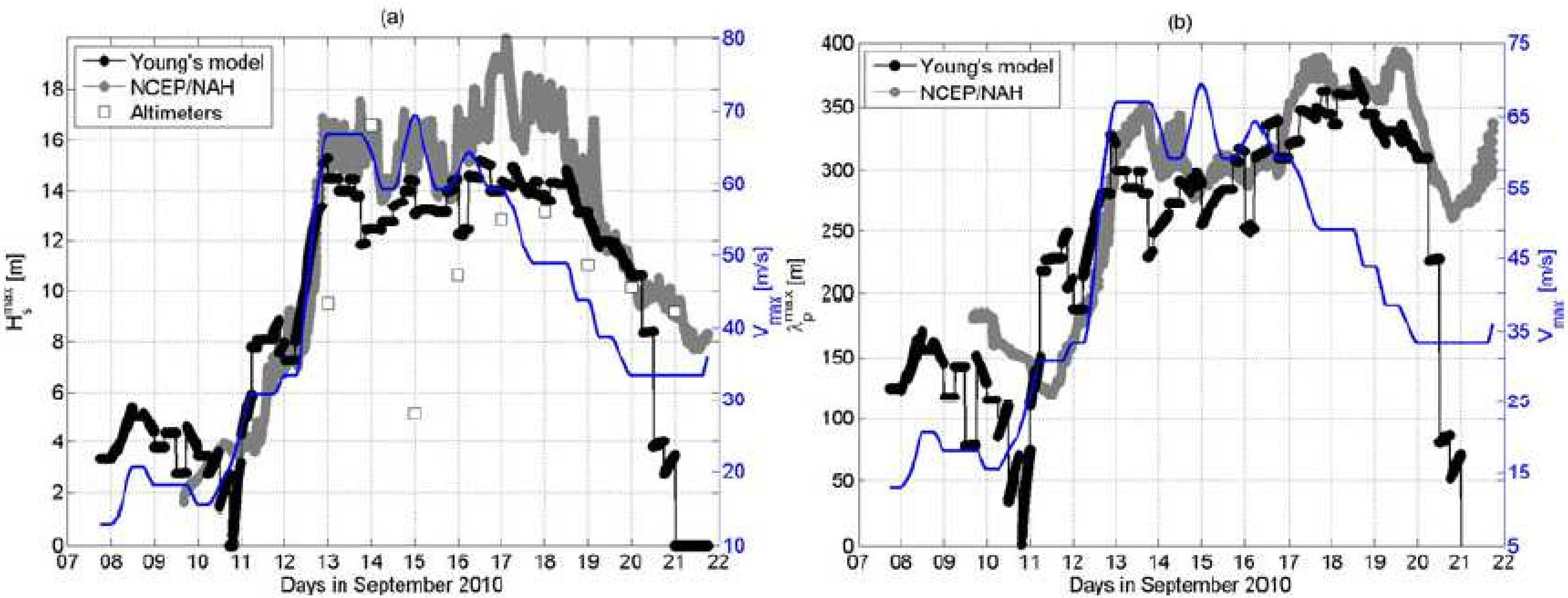

Hs>16 m

λp>300 m

Varying foam-layer thicknesses

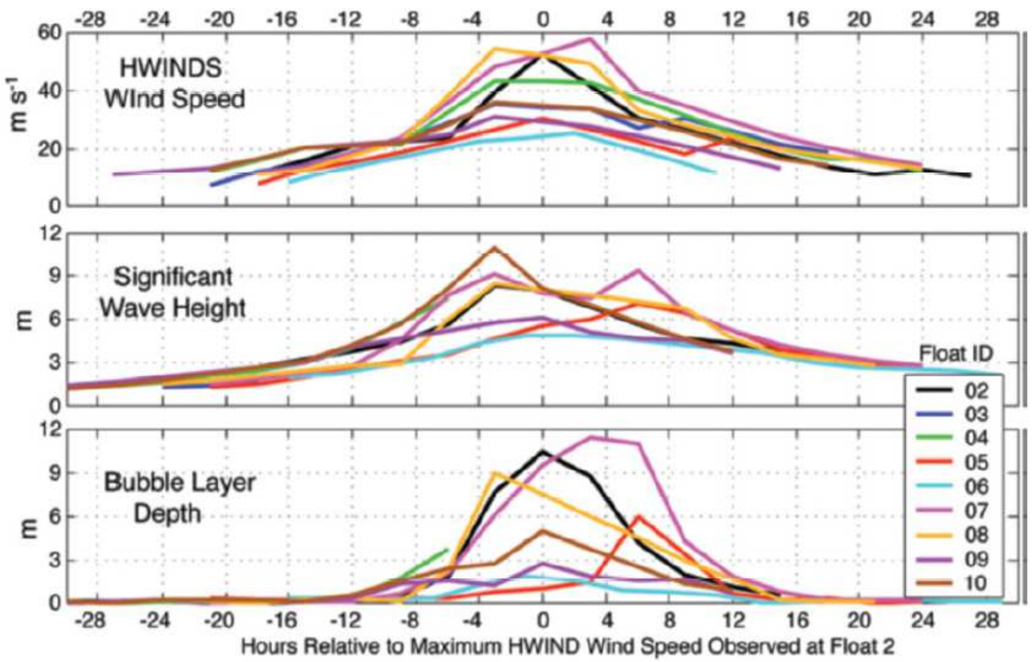

Figure 8. Significant surface wave height and bubble cloud depth measured by nine SOLO floats during hurricance Frances in 2004 and wind speed at the float location from H*WIND analysis. Time axis is hours from time of maximum wind at each float (Black et al., 2007).

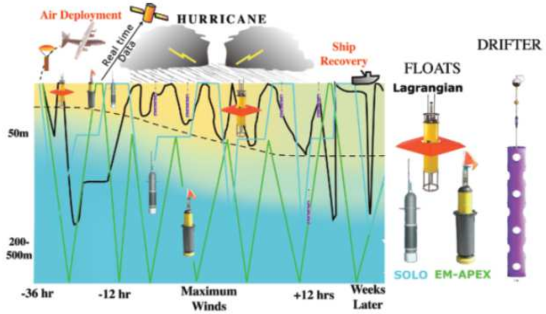

Fig. 13. Drawings of the three varieties of floats and a surface drifter as deployed into Hurricane Frances. Schematic depicts operations in Hurricane Frances (2004).

Increase of the microwave ocean emissivity
with wind speed ⇔ foam change induce effect

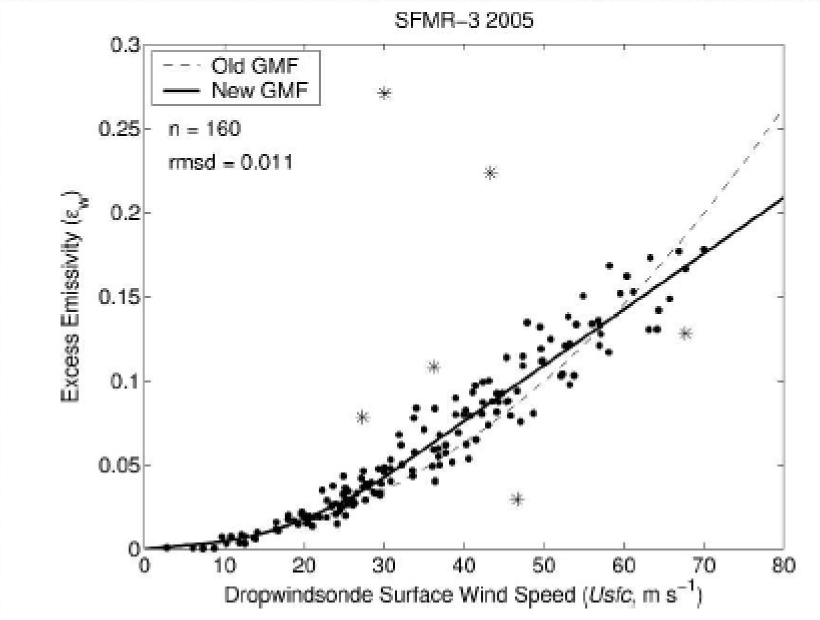

This information can be used to retrieve the surface wind speed in Hurricanes:

Principle of the Step Frequency Microwave Radiometer (SFMR) C-band:

NOAA's primary airborn sensor for measuring Tropical Cyclone surface wind speeds since 30 year (Ulhorn et al., 2003, 2007).

High winds in Hurricanes are very often associated with High rain rates

Rain Anatomy in a hurricane

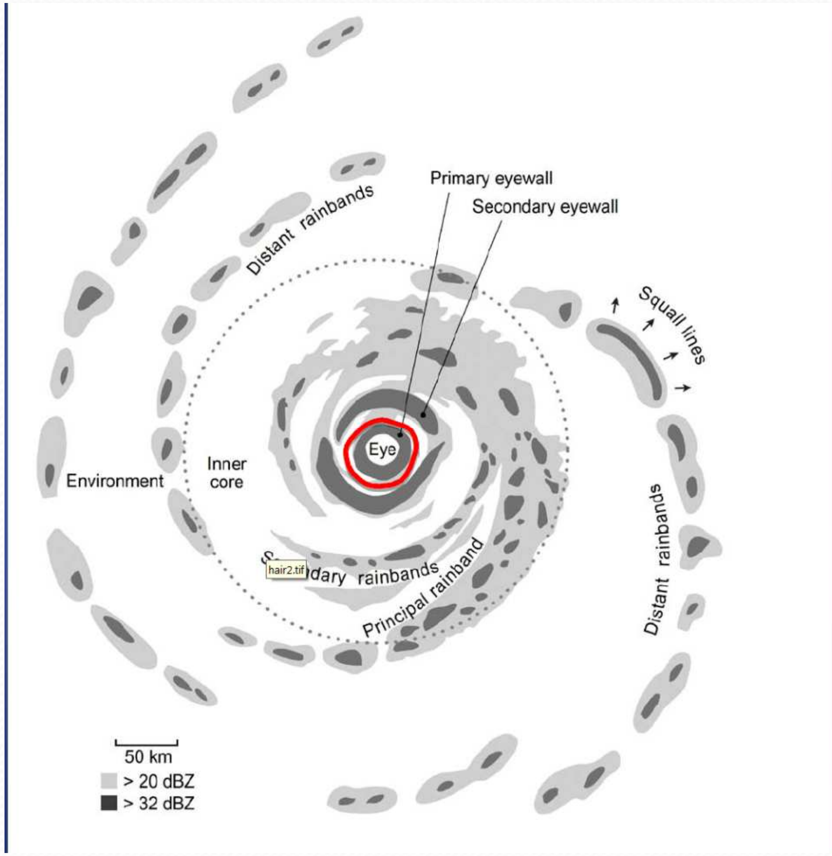

Houze 2010

Rain rate [mm/h]

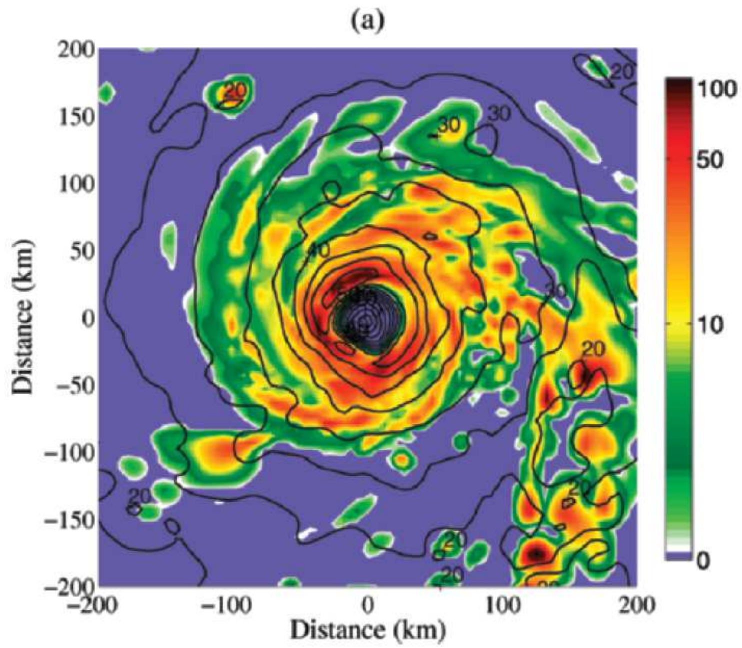

S.Shen 2007

Limitations of current satellite MW observing systems Operating at frequencies ≥ C-band

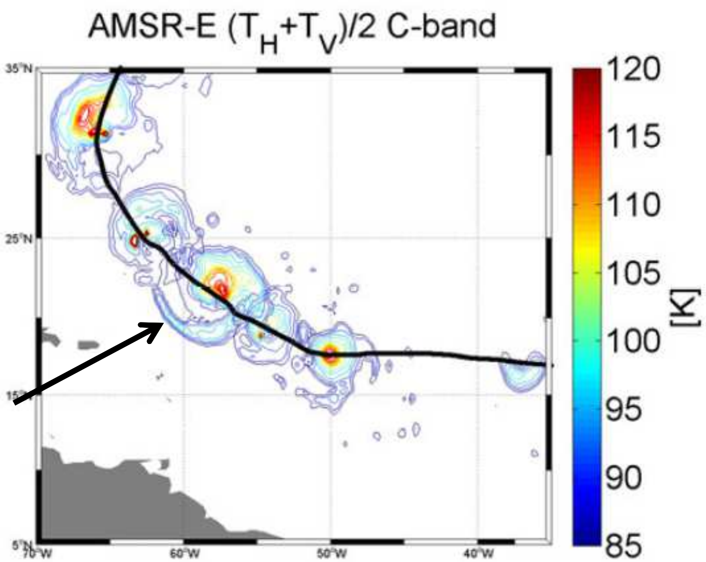

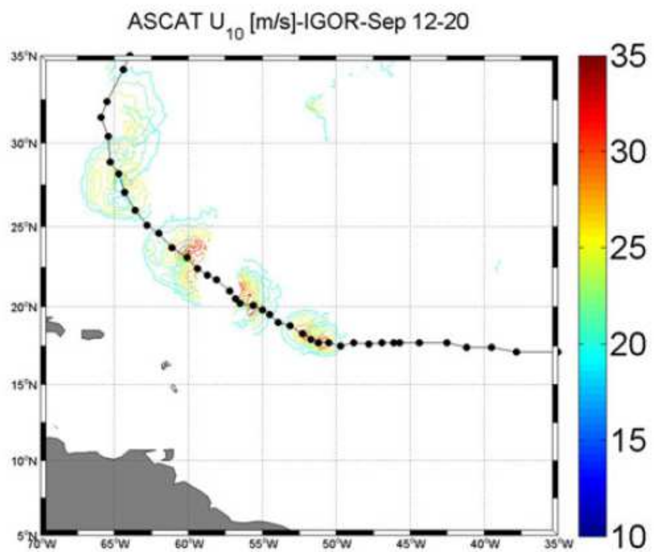

Rain Bands Signatures At C-band

- Passive/active data are strongly affected by rain for f ≥ C-band

•Radar data saturates at high winds

=>very difficult to retrieve surface winds
(for passive multiple frequency is required (SFMR))

As L-band is much less affected=>opportunity!

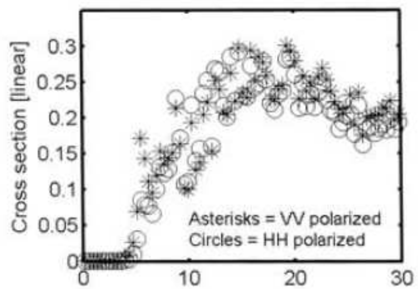

Figure 5. Normalized radar cross section (NRCS) versus centerline (0.3 m height) wind speed in the tank. Note that U_{10} is approximately $1.5U_{0.3}$.

Signatures of Tropical Cyclones in 2010 SMOS data

HURRICANE
DANIELLE

SMOS Residual (Tx+Ty)/2 for Aug 25 21:33 [K] (AF)

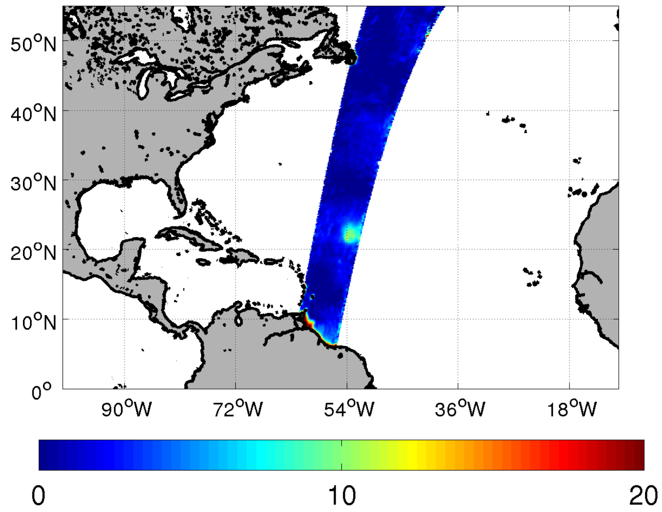

SMOS Residual (Tx+Ty)/2 for Aug 27 21:55 [K] (AF)

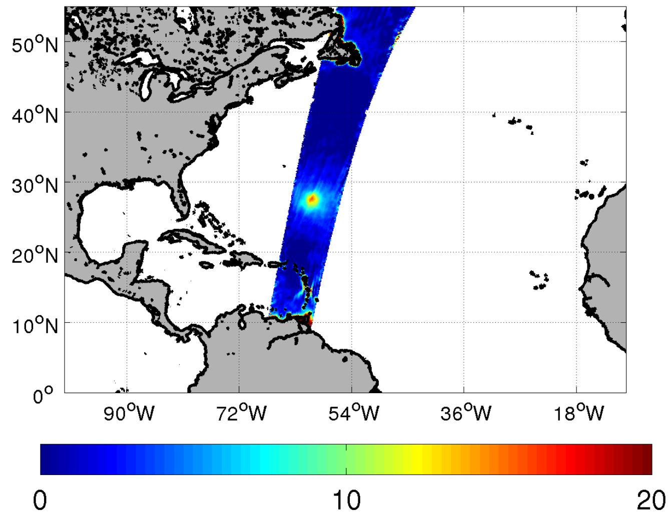

HURRICANE
EARL

SMOS Residual (Tx+Ty)/2 for Sep 02 23:01 [K] (AF)

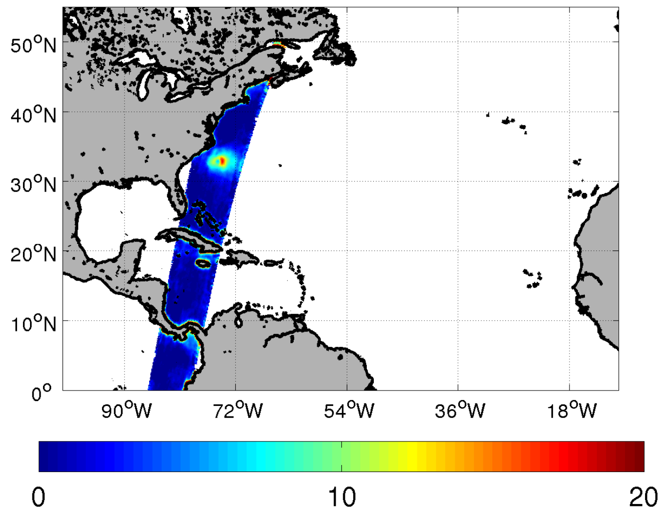

SMOS Residual (Tx+Ty)/2 for Sep 03 09:52 [K] (AF)

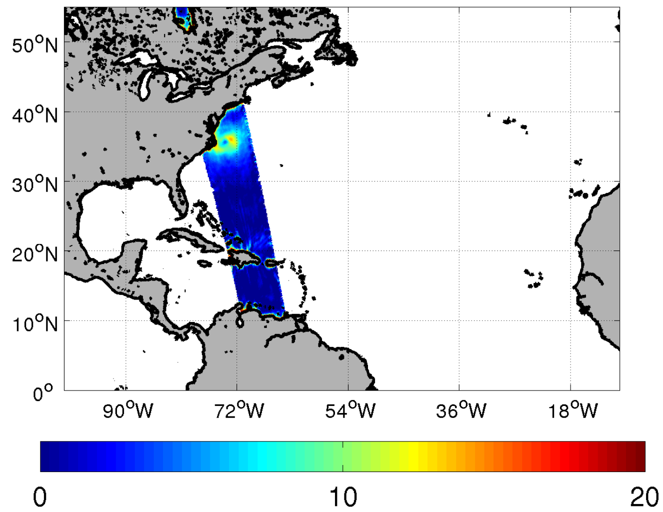

Signatures of Tropical Cyclones in 2010 SMOS data

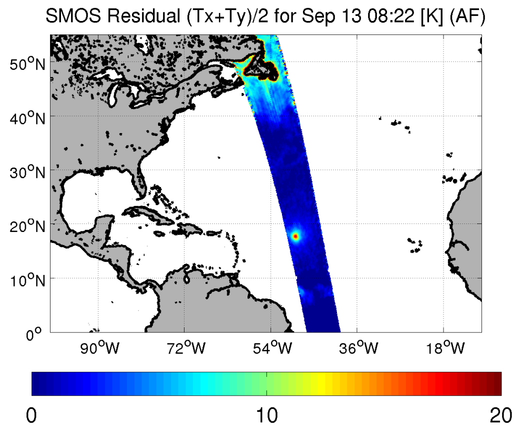

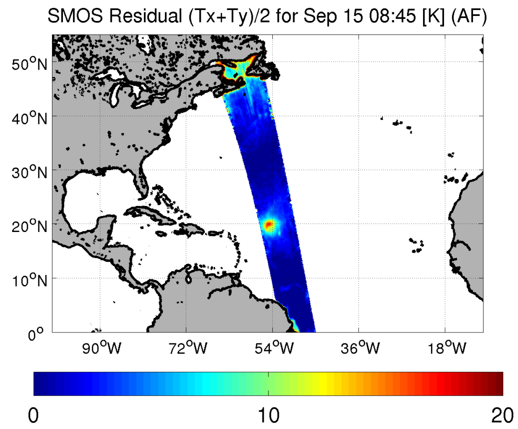

HURRICANE IGOR

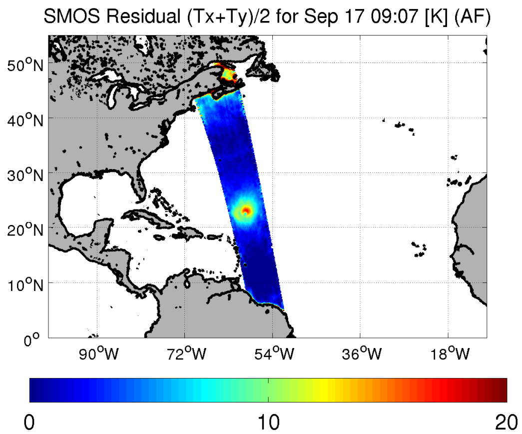

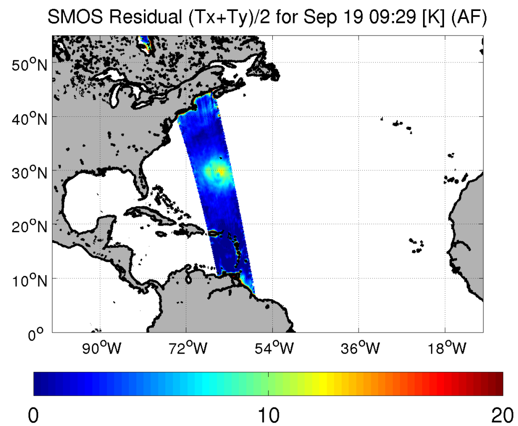

TROPICAL STORM JULIA

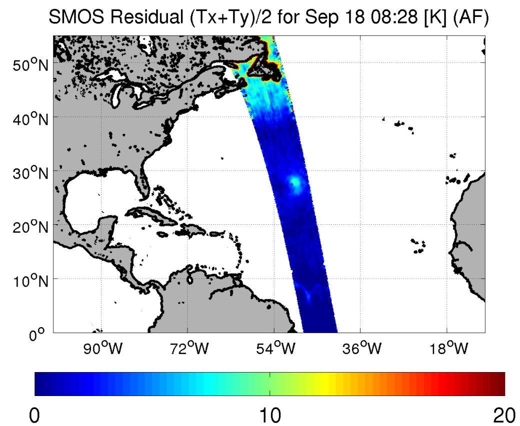

Current Understanding of

L-band radiometry in High winds:

A review:

Sensitivity of L-band emissivity to foam: FROG Campaign

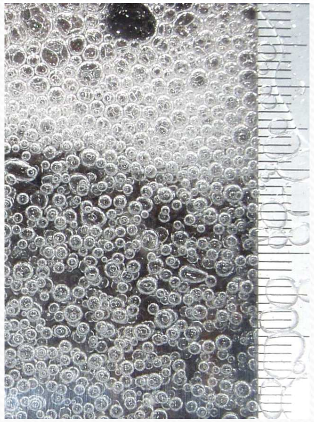

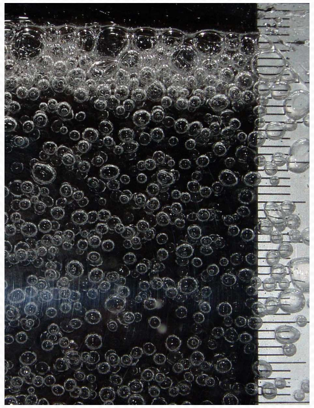

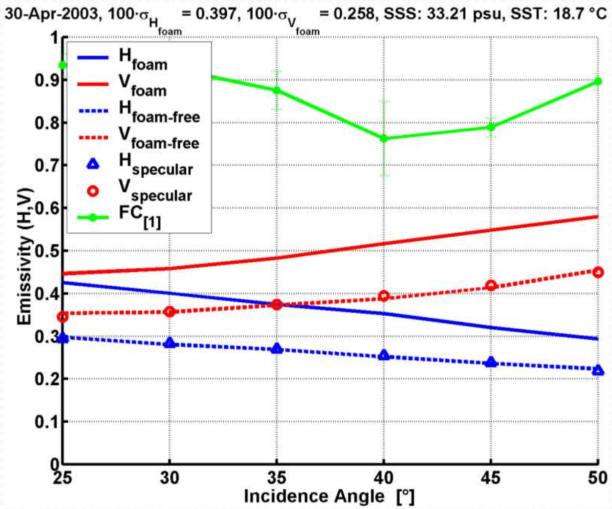

$$e_{h,v}^{Total}(\theta) = F \cdot e_{h,v}^{Foam}(\theta) + [1 - F] \cdot e_{h,v}^{Water}(\theta)$$

At 37 psu salt water the foam-induced emissivity increase is 0.007 per mm of foam thickness (extrapolated to nadir), increasing with increasing incidence angles at vertical polarization, and decreasing with increasing incidence angles at horizontal polarization.

A.Camps, et al, "*The Emissivity Of Foam-Covered Water Surface at L-Band: Theoretical Modeling And Experimental Results From The Frog 2003 Field Experiment", IEEE TGRS*, vol 43, No 5, pp 925-937, 2005.

Foam emissivity Modeling

multilayer emissivity

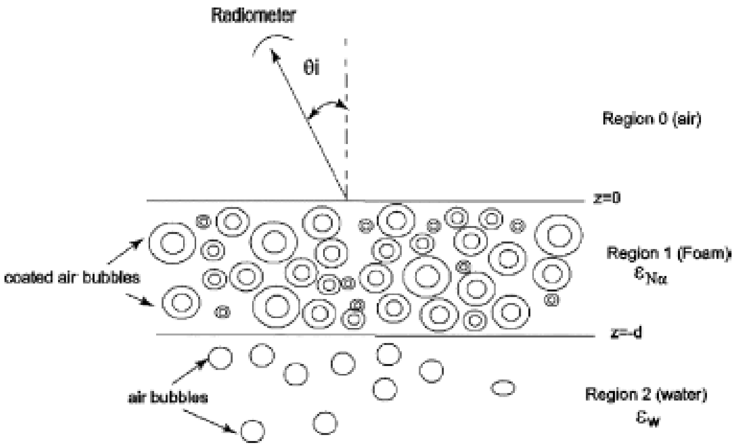

Fig. 1. Geometrical configuration for thermal emission from foam-covered ocean. The foam layer is region 1 and is absorptive and scattering. Region 2 is air bubbles embedded in sea water and is absorptive (from [5]; see Fig. 3).

$$R_p(\theta_i) = \frac{R_p^{01}(\theta_i)e^{-j2\psi} + R_p^{12}(\theta_i)}{e^{-j2\psi} + R_p^{01}(\theta_i)R_p^{12}(\theta_i)}$$

Reul, 2002

Bordonskiy *et al.*

Dombrovskiy and Raizer

"*Microwave model of a two-phase medium at the ocean surface*", *Izvestiya, Atmospheric and Oceanic Physics*, vol. 28, no. 8, pp. 650.656, 1992.

effective dielectric constant $\varepsilon_{N\alpha}$

$$\varepsilon_{N\alpha} = \frac{1 + \frac{8}{3}\pi\overline{N \cdot \alpha(r)}}{1 - \frac{4}{3}\pi\overline{N \cdot \alpha(r)}}$$

where

$$\overline{N \cdot \alpha(r)} = \frac{\kappa \int \alpha(r)p_f(r)dr}{\frac{4}{3}\int r^3 p_f(r)dr}$$

dipole approximation model

At L-band

the contribution of *multipole moment* occur for bubbles' radius on the order of 10 cm.

Comparison Foam-layer emissivity model at L-band and FROG data

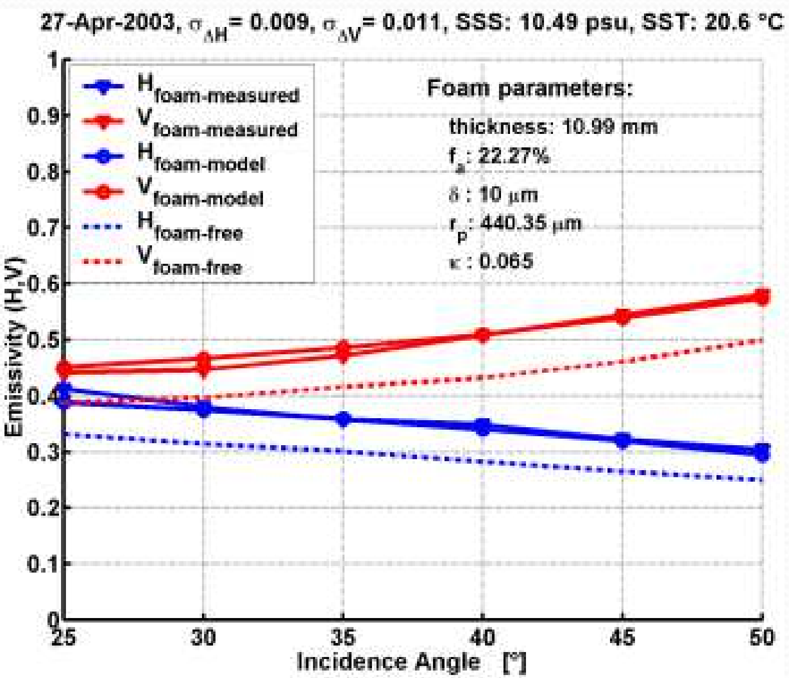

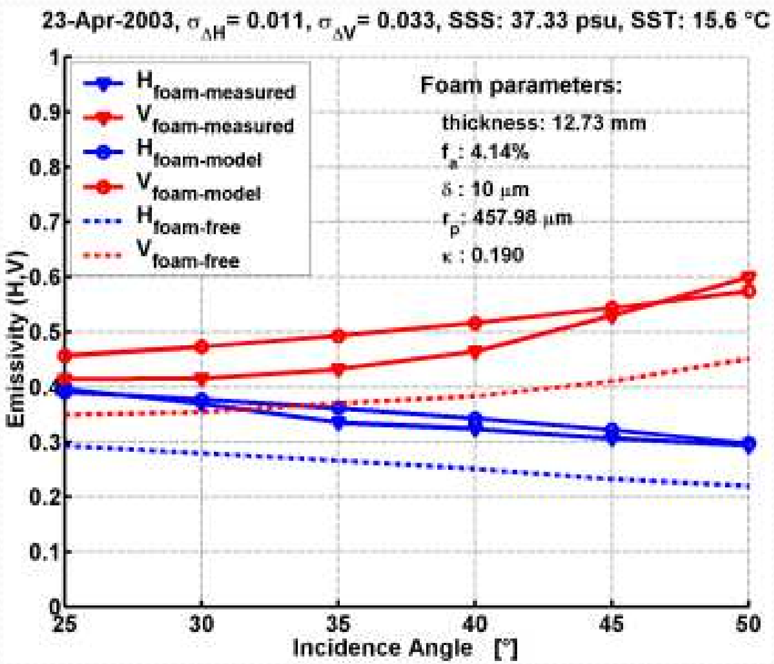

At H-polarization the agreement is excellent,

At V-polarization, the measured values show a larger variation with incidence angle

See A.Camps, et al, "*The Emissivity Of Foam-Covered Water Surface at L-Band: Theoretical Modeling And Experimental Results From The Frog 2003 Field Experiment", IEEE TGRS*, vol 43, No 5, pp 925-937, 2005.

Coverage and thickness weighted Foam-layer emissivity model

The contribution of foam formations to sea surface brightness temperature as function of wind speed *U* is given by:

$$T_{Bf}(\theta, p, f, U) = \int F(U, \bar{\delta}) \cdot T_s \cdot e_{Bf}^{typ}(\theta, p, f, \bar{\delta}) d\bar{\delta}$$

Where

•*f*, *p* and θ are the receiving electromagnetic frequency, polarization and incidence angle of the radiometer respectively,

•*F(U, δ)* is the fraction of sea surface area covered by whitecaps with thickness δ at *U*,

•T_s is the physical tempearture of foam, usually assumed the same as the bulk sea surface temperature and,

•e^{typ}_{Bf} is the emissivity of typical sea foam-layer.

•N.Reul and B. Chapron, "*A model of sea-foam thickness distribution for passive microwave remote sensing applications*", *J. Geophys. Res.,* 108 (C10), Oct, 2003.

Coverage and thickness weighted Foam-layer emissivity model

$$e_B = e_{spec} + \underbrace{[\Delta e_{rough} + \Delta e_{whitecaps}]}_{wind-induced}$$

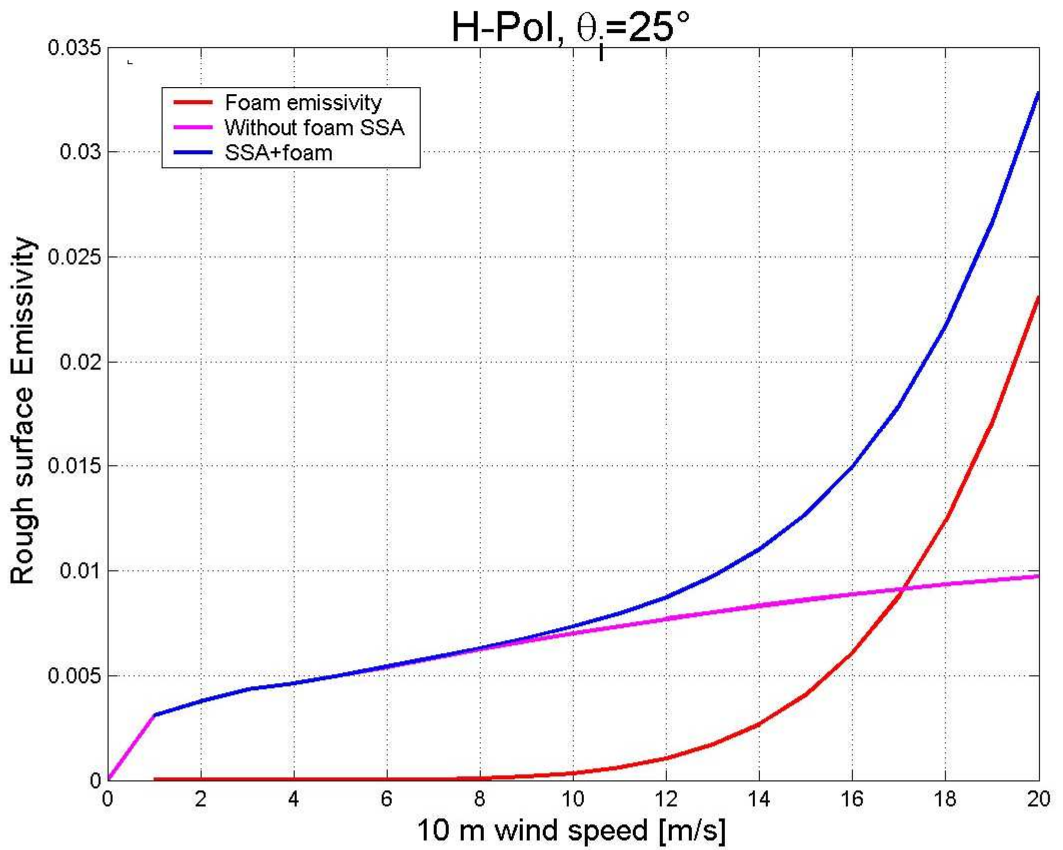

Airborn Campaign with PALS during a storm in 2010

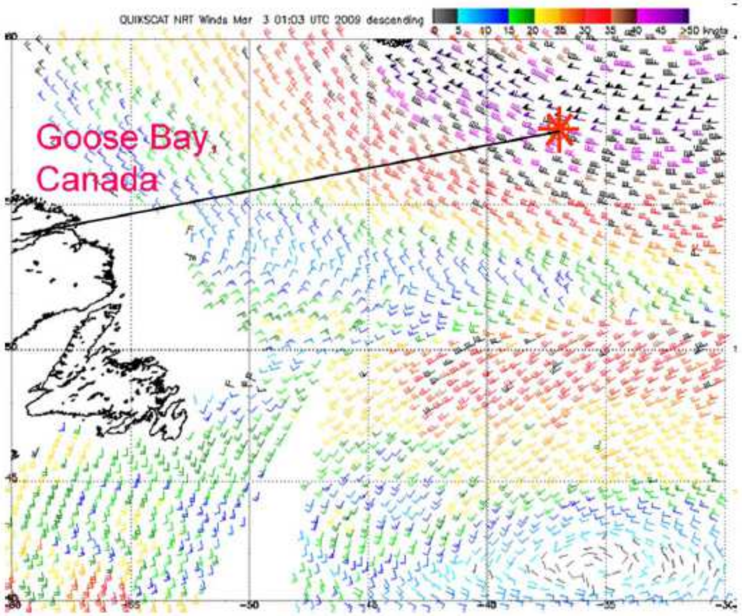

Fig. 1. NASA P-3 flight track from Goose Bay, Canada, to the selected way point in the North Atlantic. Near the way point, we performed the star-pattern, wing wag, and circle flights.

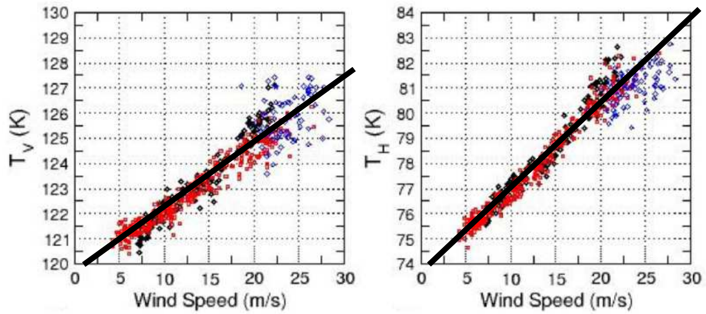

Fig. 13. V and H brightness temperatures taken at a 45° incidence angle from the star pattern (blue), inbound (red), and outbound (black) tracks on March 2, 2009, are plotted versus the wind speed derived from the POLSCAT measurements. All brightness temperature measurements have been translated to a 45° incidence angle and corrected for galactic radiation.

Linear increase of Tb with wind
Up to 28 m/s

Weak incidence angle dependence
At high winds

Yueh S.H., S.J. Dinardo, A.G. Fore, F.K. Li (2010), "Passive and Active L-band Microwave Observations and Modeling of Ocean Surface Winds", IEEE Trans. Geosci. Remote Sens., vol. 48, no. 8, pp. 3087-3100.

Wind Excess Emissivity at High winds

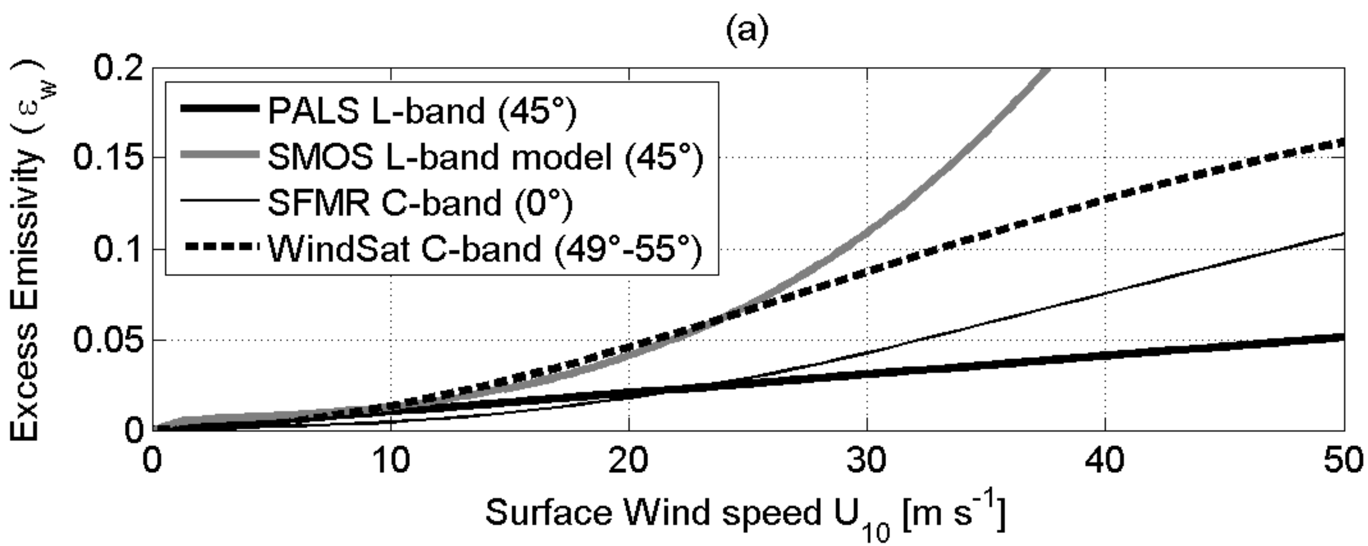

According to PALS sensitivity ~0.35K/m/s for the First Stokes parameter/2

C-band TB~3 times more sensitive to wind speed than L-band

SMOS L-band model overestimates the Tb increase with wind for U>12 m/s

Rain attenuation at L-band

Because of the small ratio of raindrop size to the SMOS electromagnetic wavelength (~21 cm), scattering by rain is almost negligible at L-band, even at the high rain rates experienced in hurricanes.

Rain impact at 1.4 GHz can be approximated entirely by absorption and emission (Rayleigh scattering approximation valid)

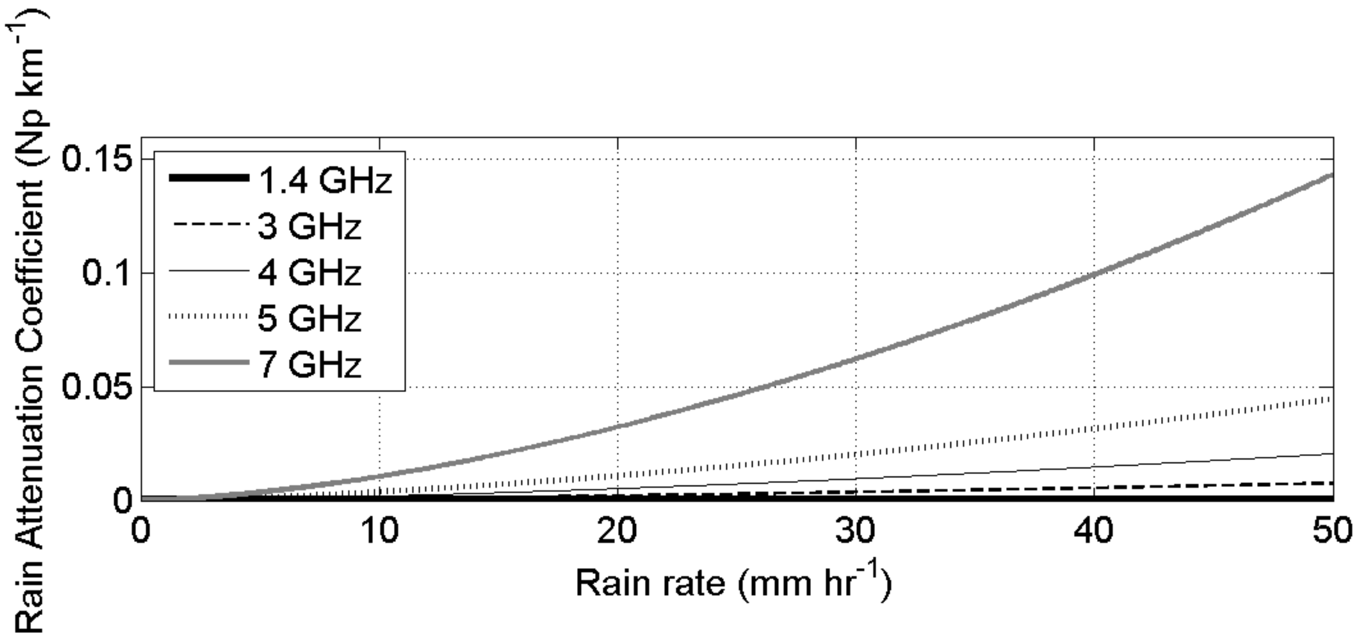

Generally two order of magnitude smaller at L-band (1.4 GHz) than at C-band (5-7 GHz)

Potential rain impact at L-band

At L-band, increase in Tb due to rain is simply proportional to the total content of liquid water **Wentz F. J.** (2005), **Skou N. and D. Hoffman-Bang** (2005),

$$\Delta T_{B,liq} = 2(1-E)\bar{T}_{liq}\,\bar{a}_{ray}\,L\sec\theta$$

E: surface emissivity

$\bar{T}_{liq}$:average temperature of the rain cloud

$\bar{a}_{ray}$: Rayleigh coefficient at temperature $\bar{T}_{liq}$

L is the total content of liquid water in the field of view

Assuming a tropical rain layer thickness of 3 km, the model predict an increase in the first stokes parameter due to rain of

$\Delta T_{B,liq} =$ ~0.2 K at a rain rate of 10 mm.hr-1
~0.35 K at a rain rate of 30 mm.hr-1, (first Stokes parameter/2)

Potential rain impact at L-band in very high rain rates

RTM simulations **Schulz, J.** (2002)

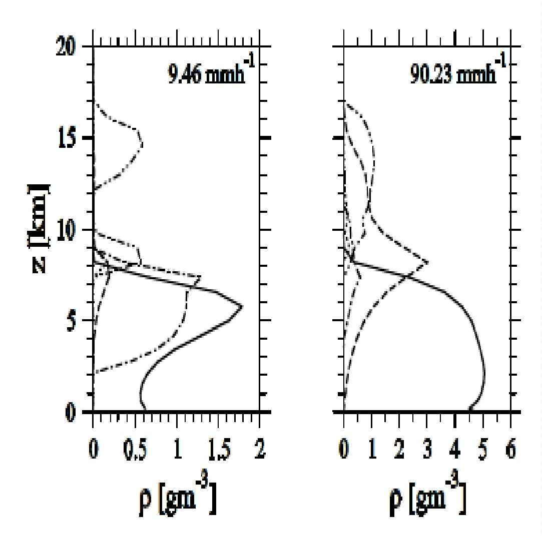

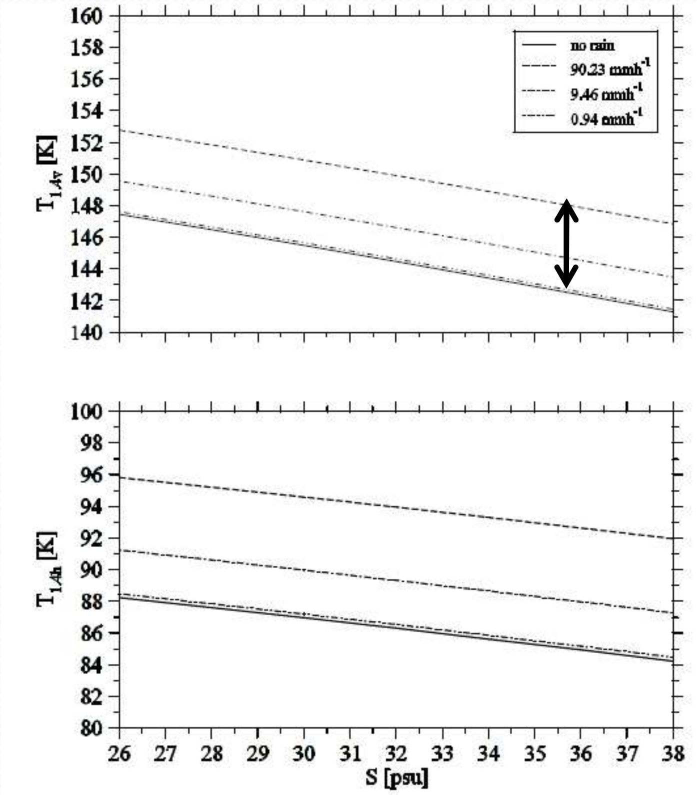

In very high rain rates ~90 mm/h=> potential significative impact

$\Delta T_{B,liq}$ = 4 K for the first Stokes parameter/2

Analysis of SMOS signature over Category 4 Hurricane IGOR

Collection of Data for analysis

Collection of Hurricane Igor data:

•SMOS L1B data corrected for all contibutions except roughness (sss=clim)

•National Hurricane Center Best Track data:

=>track; max winds, radius at 34, 50 and 64 knots

•AOML Hurricane research division

=>H*WIND observation analysis winds
=>SFMR data
•NOAA/NWS/NCEP North Atlantic Hurricane Wind Wave forecasting system (NAH):

=>Wave parameters

•NOAA/Geophysical Fluid Dynamic Laboratory (GFDL) hurricane model winds
•ECMWF
•ASCAT
•SSM/I, WindSAt

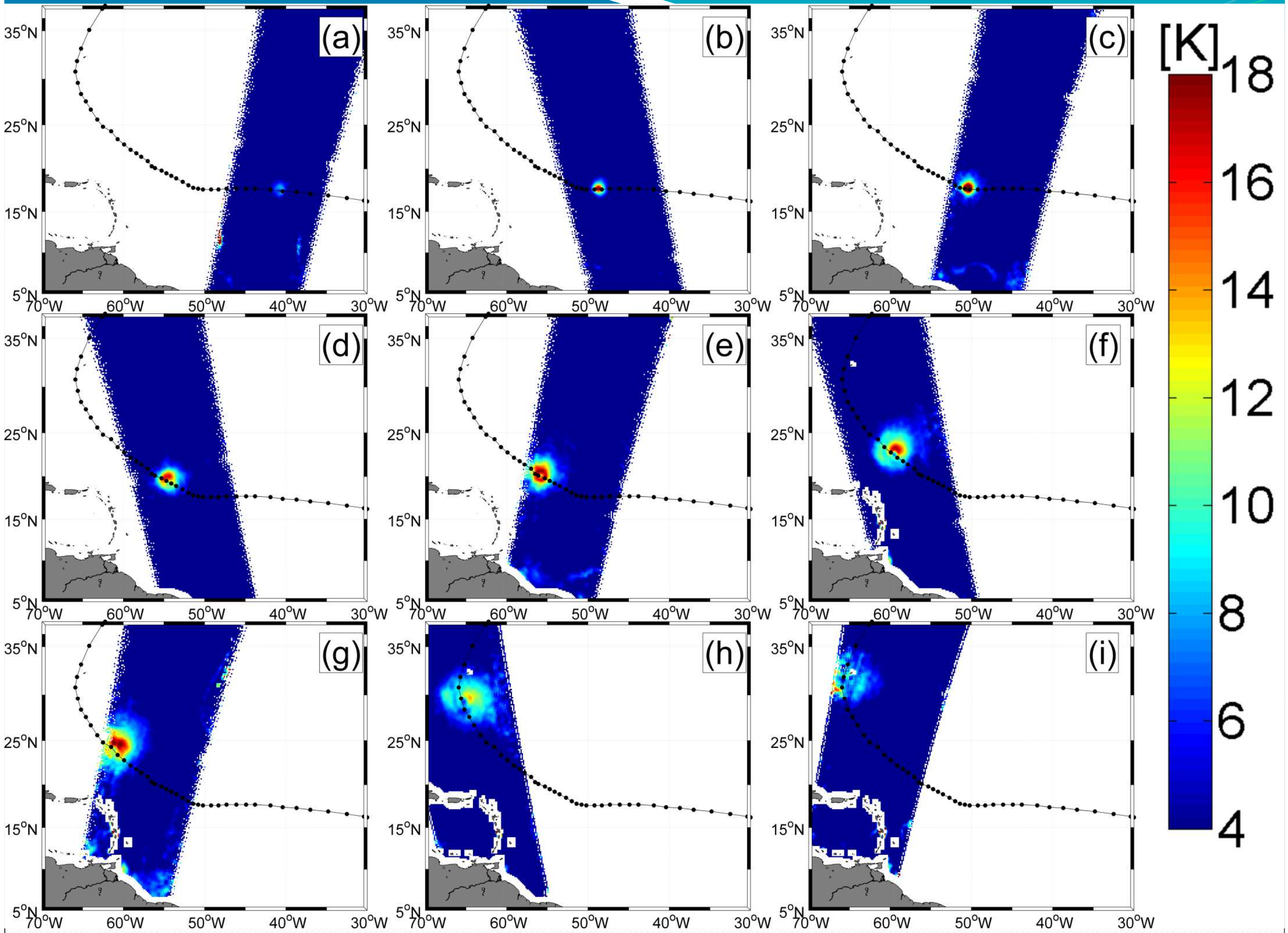

(a)
(b)
(c)
(d)
(e)
(f)
(g)
(h)
(i)
35°N
25°N
15°N
5°N
70°W
60°W
50°W
40°W
30°W
[K]
18
16
14
12
10
8
6
4

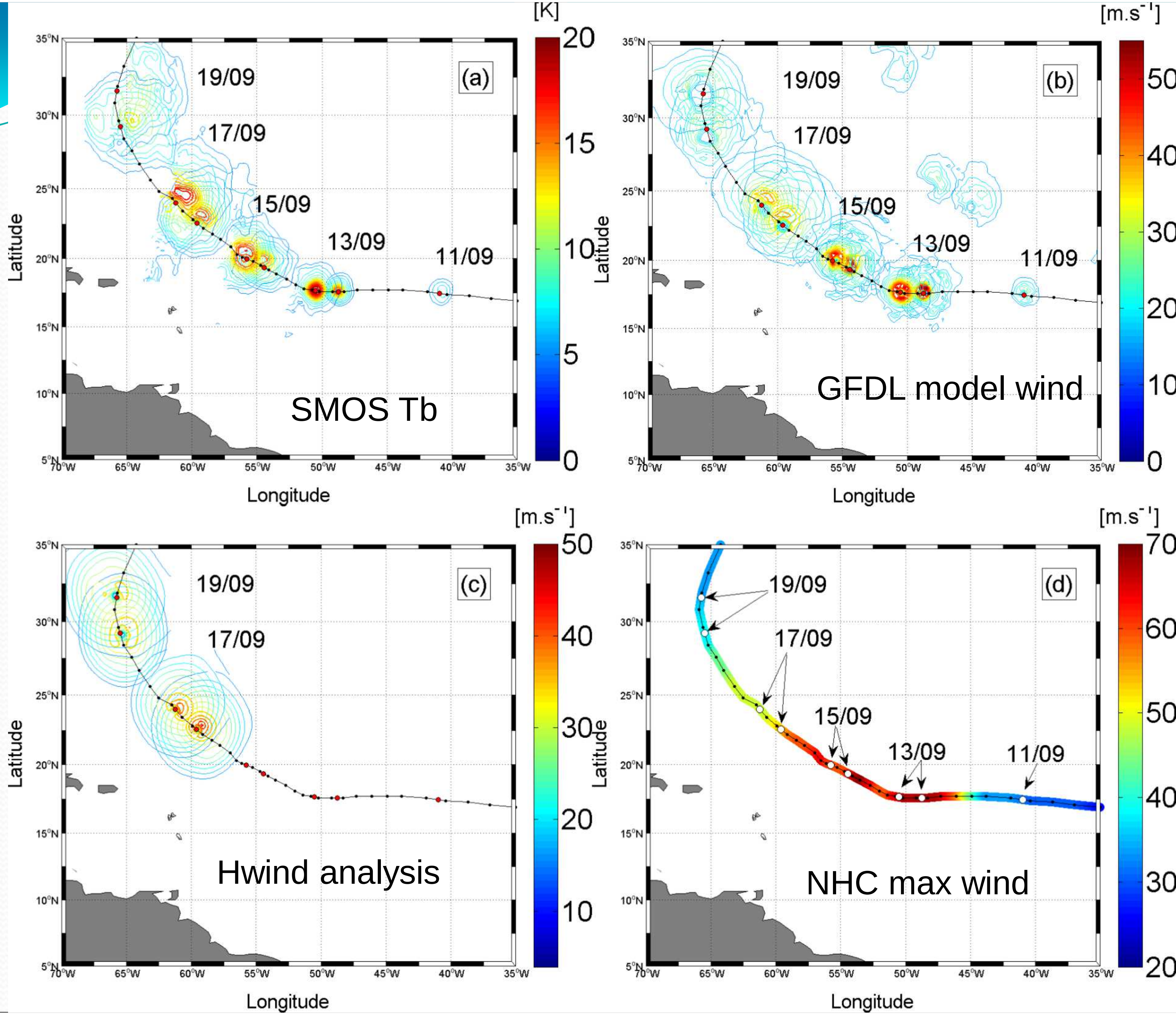

(a)
SMOS Tb
[K]
(b)
GFDL model wind
[m.s-1]
(c)
Hwind analysis
[m.s-1]
(d)
NHC max wind
[m.s-1]
19/09
17/09
15/09
13/09
11/09
Latitude
Longitude

Geophysical Model function: Tb=f(wind speed)

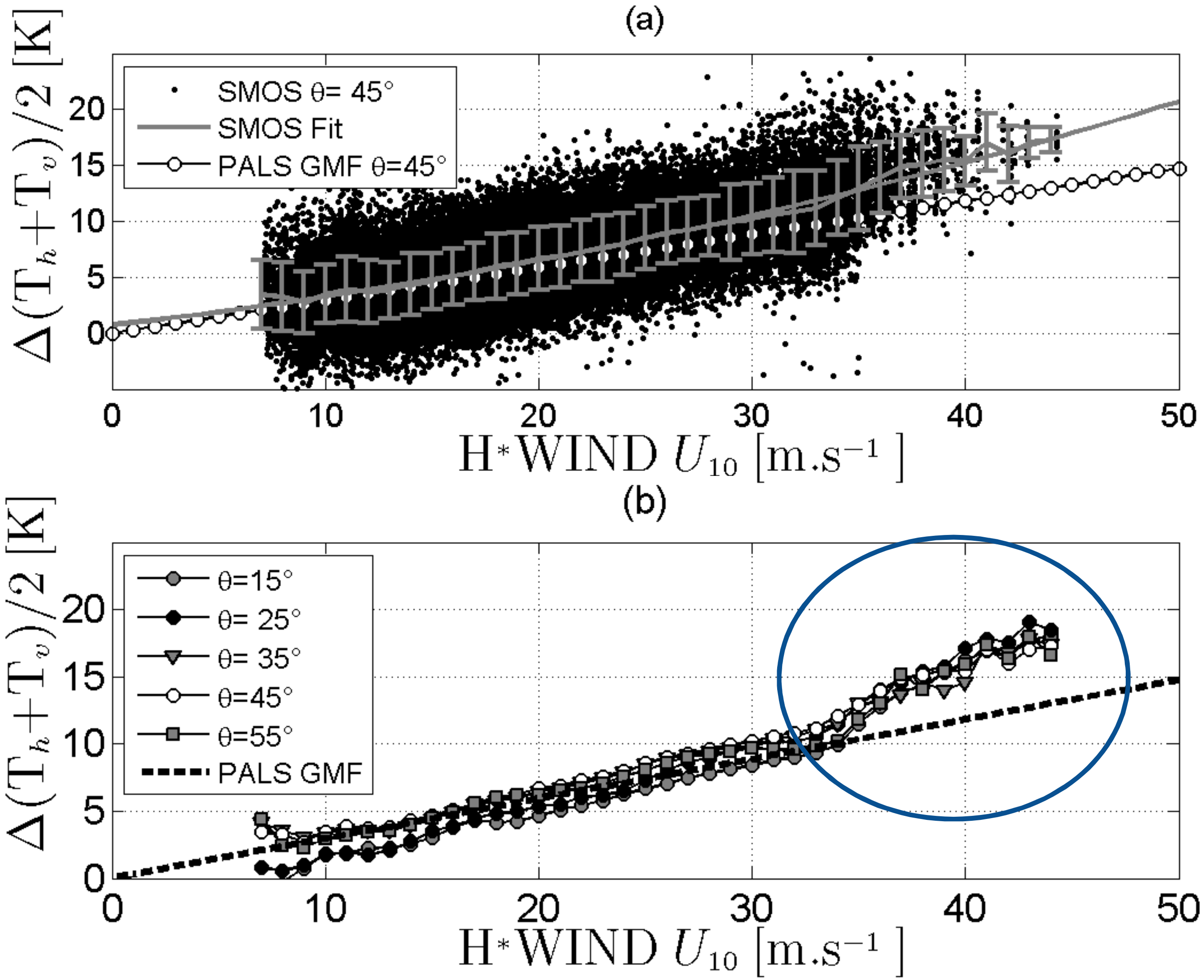

Change
of sensitivity
at
Hurricane
wind
Force (>33 m/s)

Weak Incidence
Angle dependence

Very consistent
With PALS

Geophysical Model function: Tb=f(wind speed)

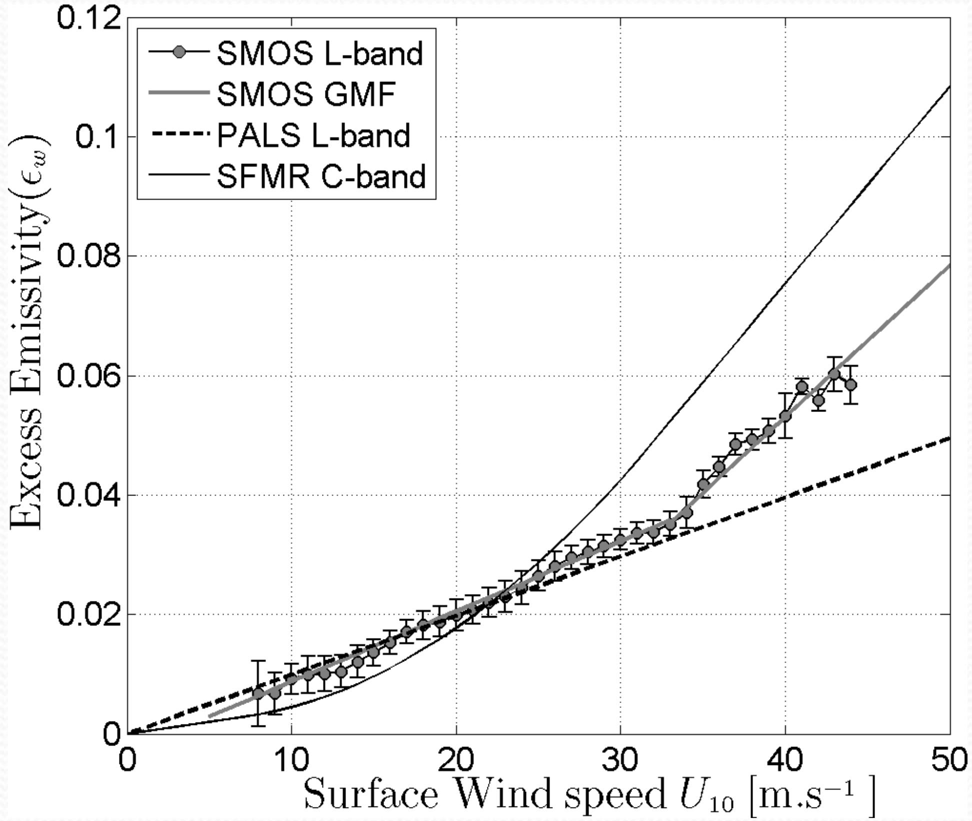

$$\Delta I = \frac{\Delta(T_H+T_V)}{2} = 0.35\,U_{10}\text{-}1.3 \qquad U_{10} \leq 33\ \text{m.s}^{-1}$$

$$= 0.75\,U_{10}\text{-}14.5 \qquad U_{10} \geq 33\ \text{m.s}^{-1}$$

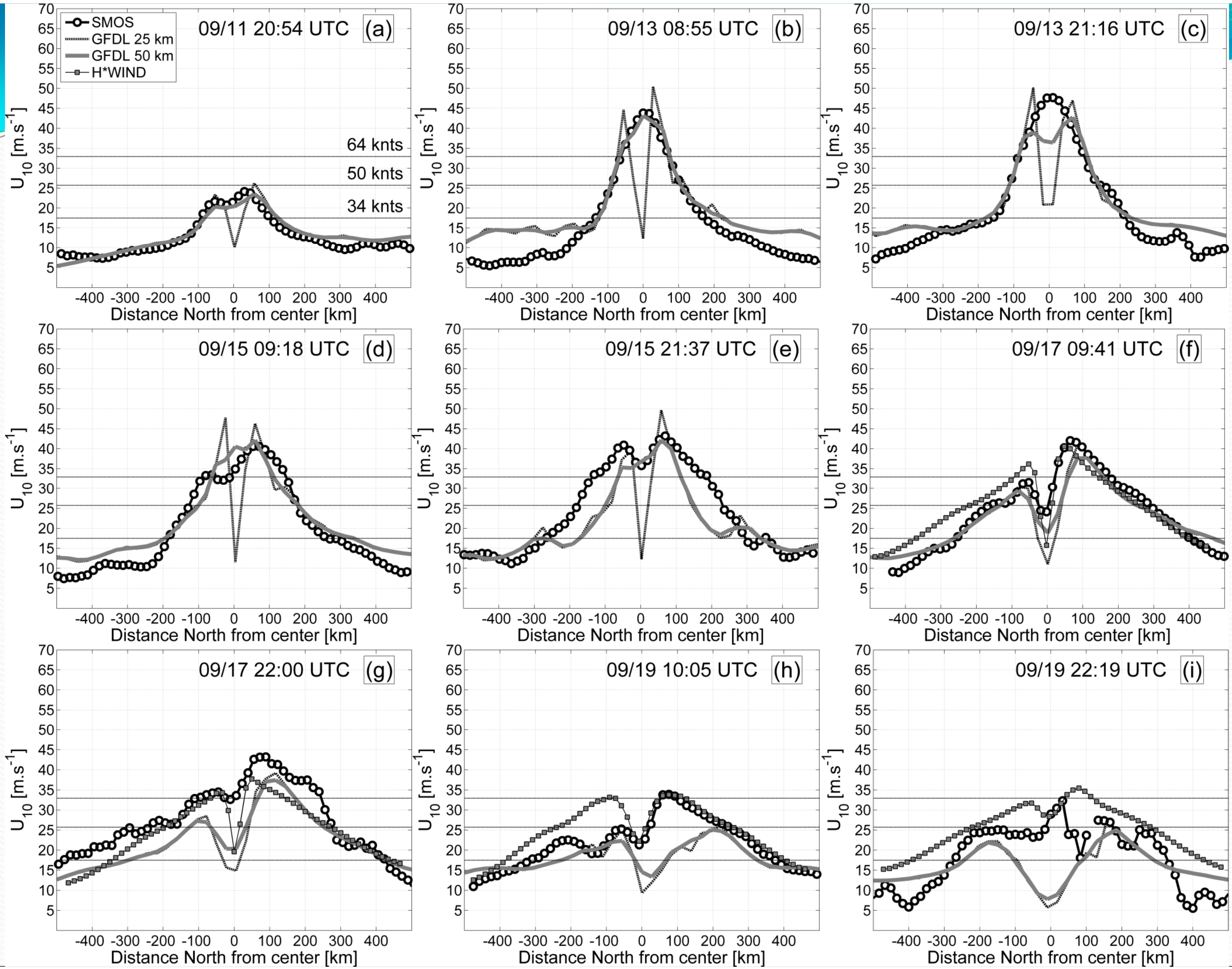

SMOS
GFDL 25 km
GFDL 50 km
H*WIND
09/11 20:54 UTC (a)
09/13 08:55 UTC (b)
09/13 21:16 UTC (c)
09/15 09:18 UTC (d)
09/15 21:37 UTC (e)
09/17 09:41 UTC (f)
09/17 22:00 UTC (g)
09/19 10:05 UTC (h)
09/19 22:19 UTC (i)
64 knts
50 knts
34 knts
U_{10} [m.s^{-1}]
Distance North from center [km]

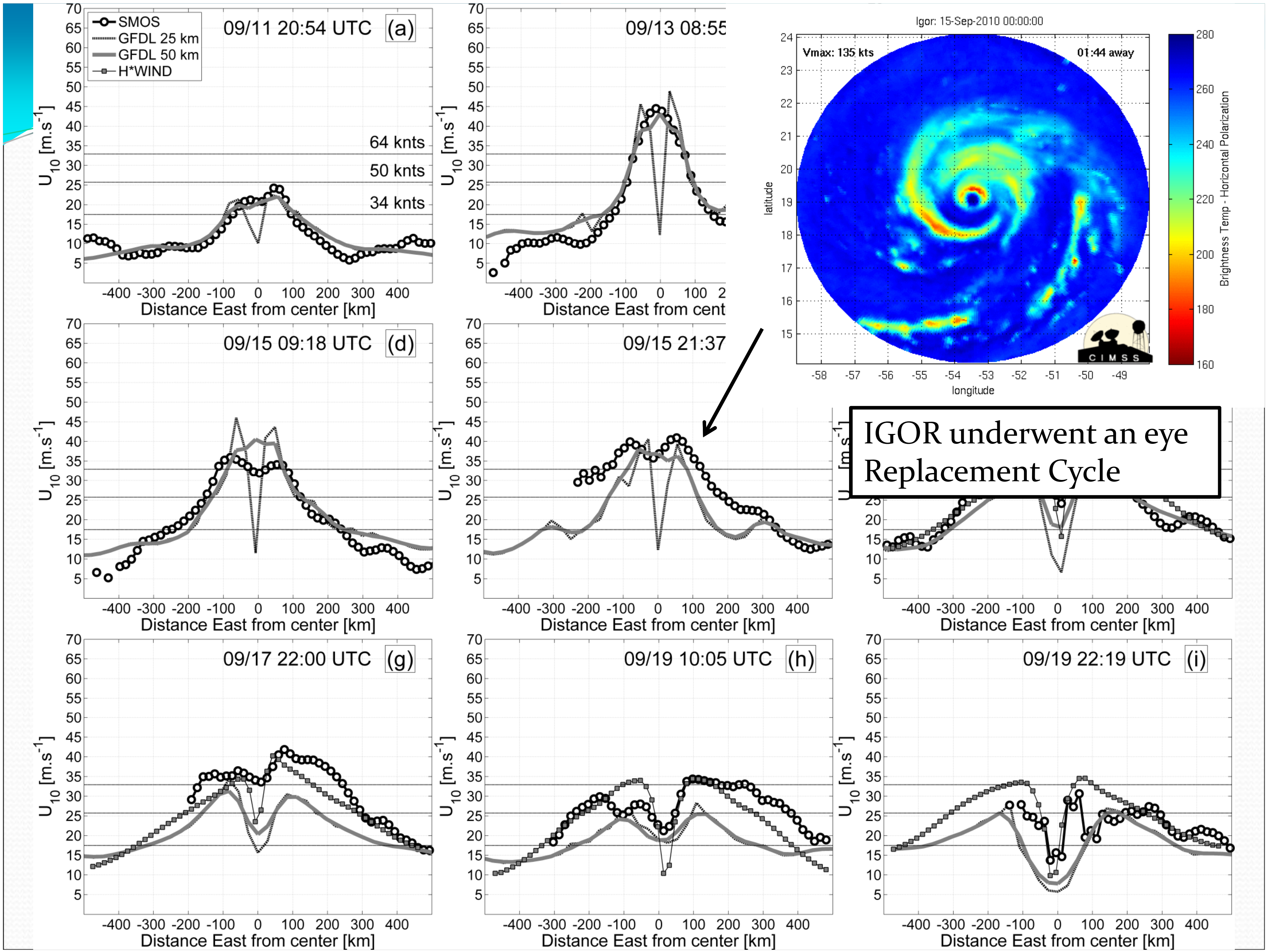

SMOS
GFDL 25 km
GFDL 50 km
H*WIND
09/11 20:54 UTC (a)
09/13 08:55
09/15 09:18 UTC (d)
09/15 21:37
09/17 22:00 UTC (g)
09/19 10:05 UTC (h)
09/19 22:19 UTC (i)
64 knts
50 knts
34 knts
U10 [m.s-1]
Distance East from center [km]
Igor: 15-Sep-2010 00:00:00
Vmax: 135 kts
01:44 away
latitude
longitude
Brightness Temp - Horizontal Polarization
CIMSS
IGOR underwent an eye Replacement Cycle

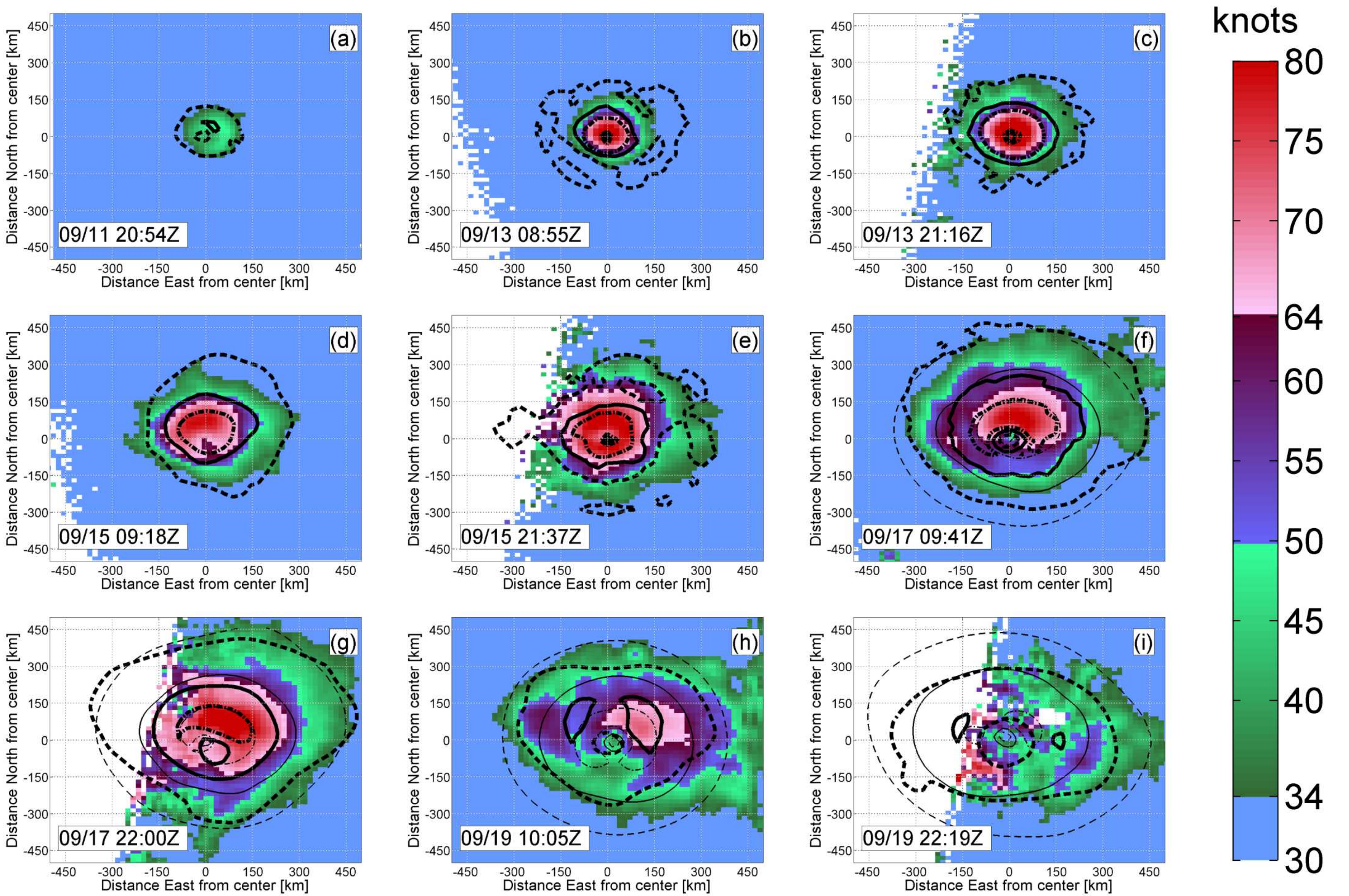
knots
80
75
70
64
60
55
50
45
40
34
30
(a)
09/11 20:54Z
(b)
09/13 08:55Z
(c)
09/13 21:16Z
(d)
09/15 09:18Z
(e)
09/15 21:37Z
(f)
09/17 09:41Z
(g)
09/17 22:00Z
(h)
09/19 10:05Z
(i)
09/19 22:19Z
Distance North from center [km]
Distance East from center [km]
-450 -300 -150 0 150 300 450

Wind field Structure from SMOS

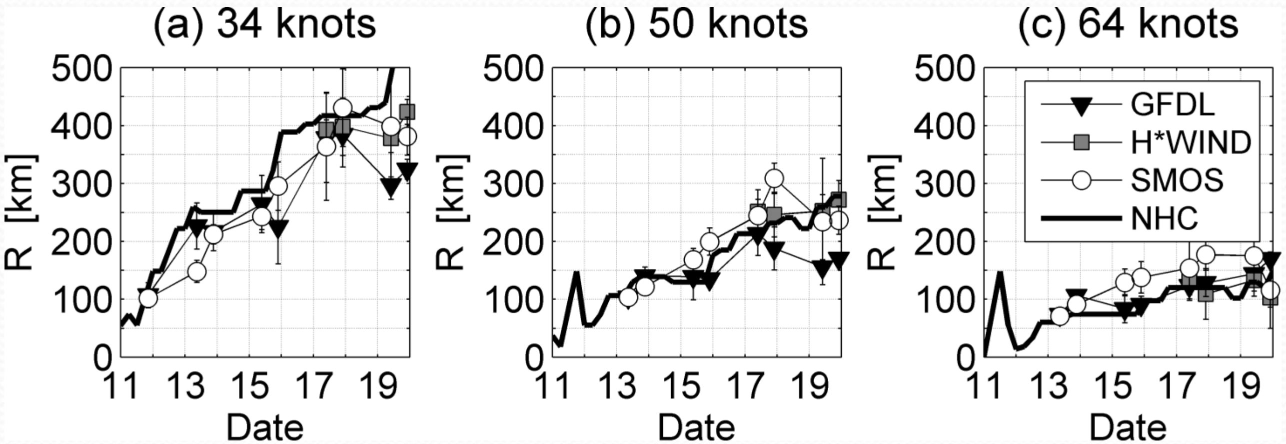

Radius of wind speed larger than 34, 50 and 64 knots

Maximum Wind estimates from SMOS

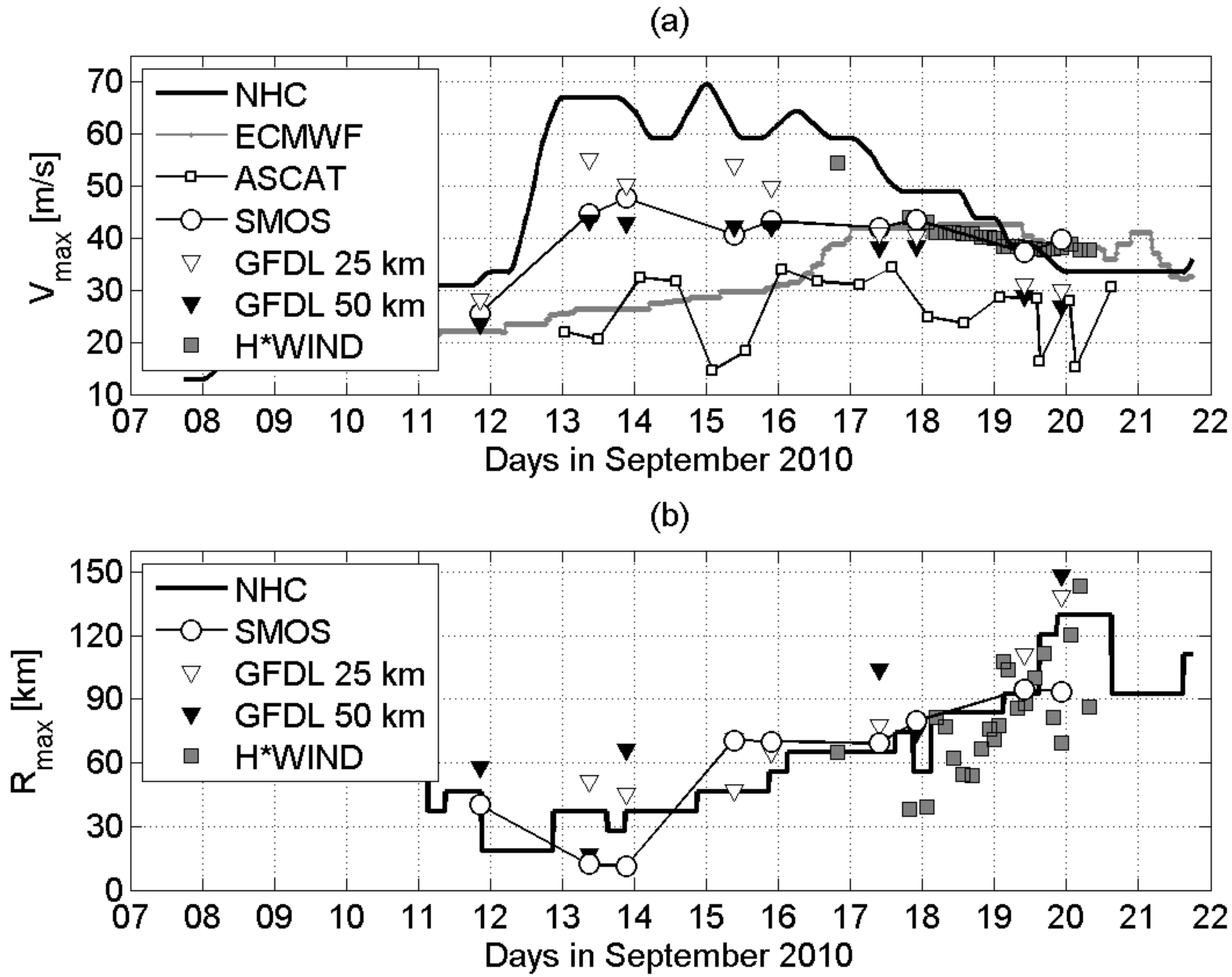

SMOS clearly outperform ASCAT in that case

Comparison at SFMR transects

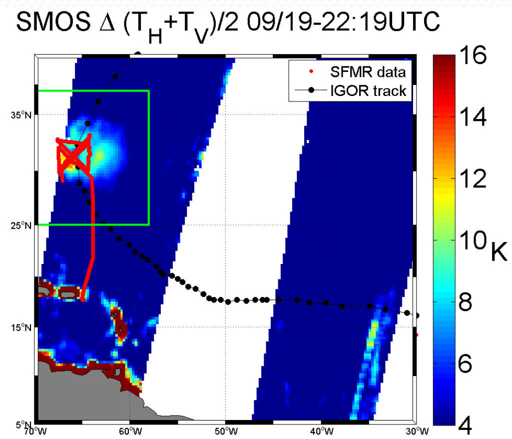

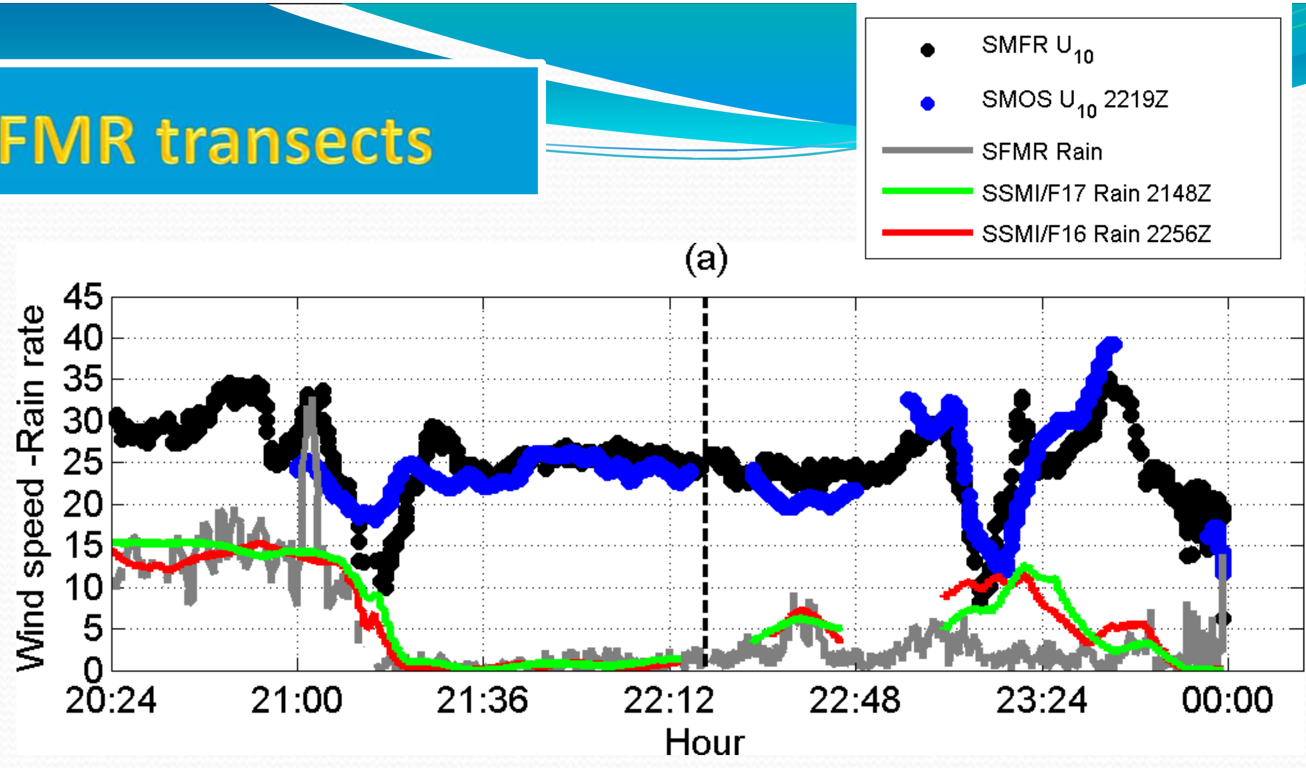

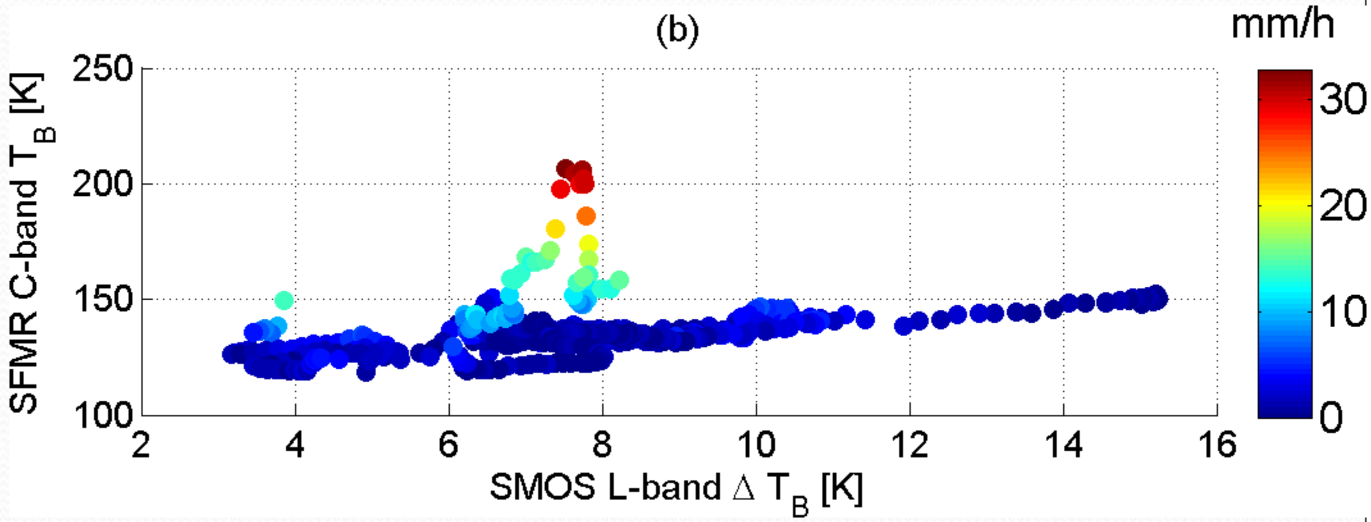

Potential rain Impact

windSat rain Rate exactly at the same time than SMOS

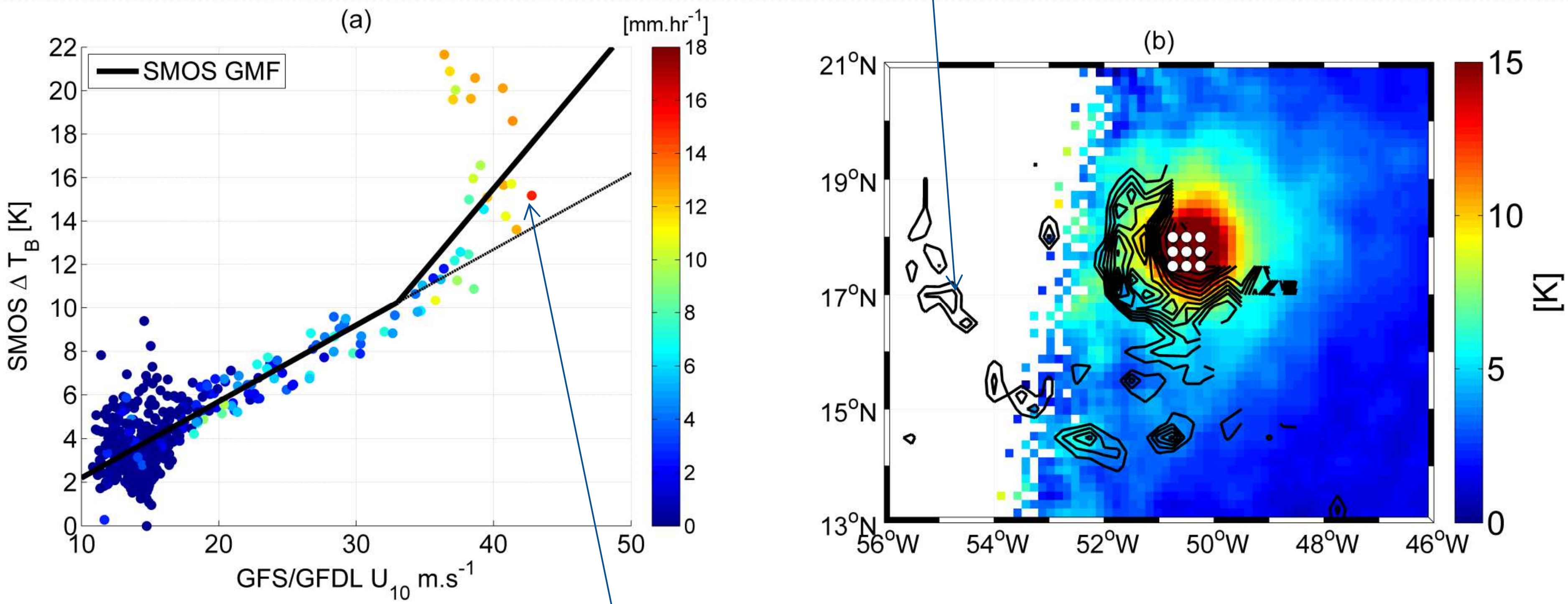

No clear signature correlated with highest rain rates here

Perspectives

Paper in revision for JGR ocean:

"SMOS satellite L-band radiometer: a new capability for ocean surface remote sensing in Hurricanes", N.Reul, J.Tenerelli, B.Chapron, D.Vandemark, Y.Quilfen and Yann Kerr, submitted to JGR Ocean, 2011.

Analysis of a larger data set for year 2010-2011

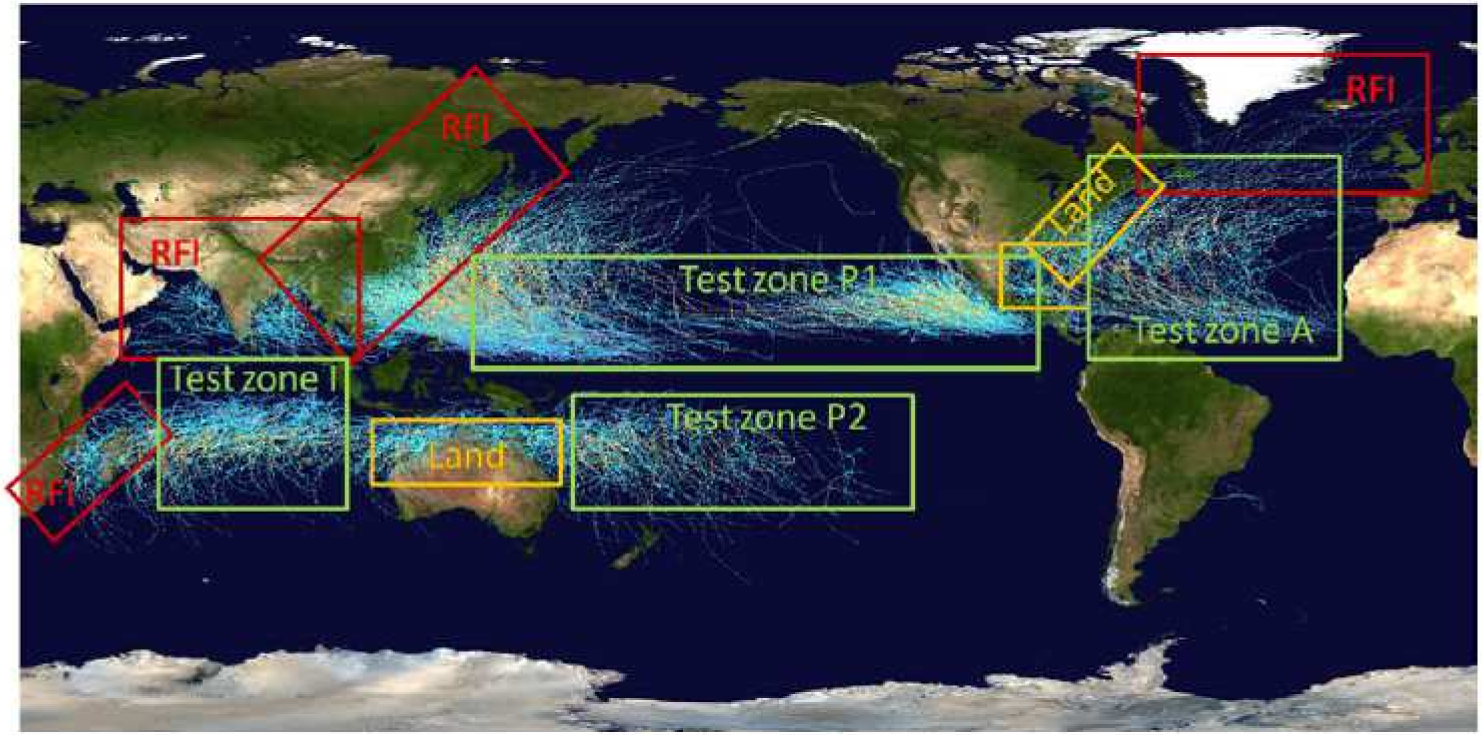

Figure 11: Map showing the tracks of all Tropical cyclones which formed worldwide from 1985 to 2005 (NASA). In Red: area for which Radio Frequency Interference strongly contaminate SMOS data, in orange, zones for which potentially strong land contamination is expected. In green: potential test zones.

2010 09 21 22 : malakas, fanapi,megi,

Main limitation of SMOS for Hurricane=> RFI and spatial-resolution

Salinity and Wind retrieval from L-band sensors: a promising synergy for Hurricane study

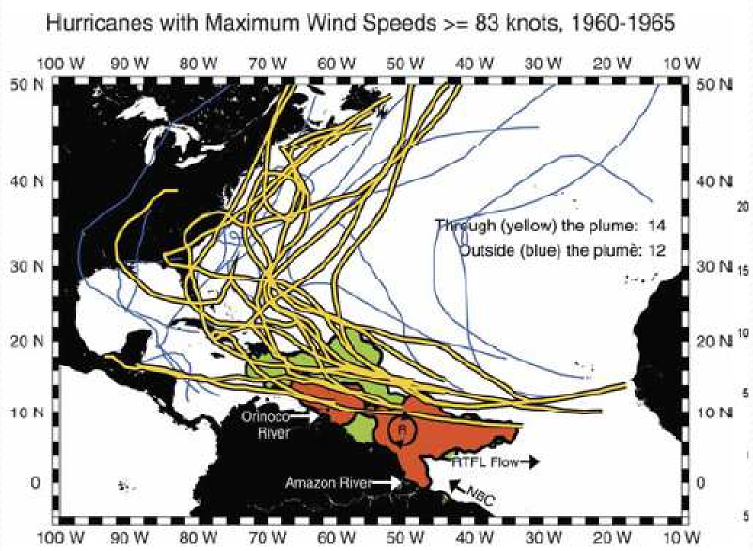

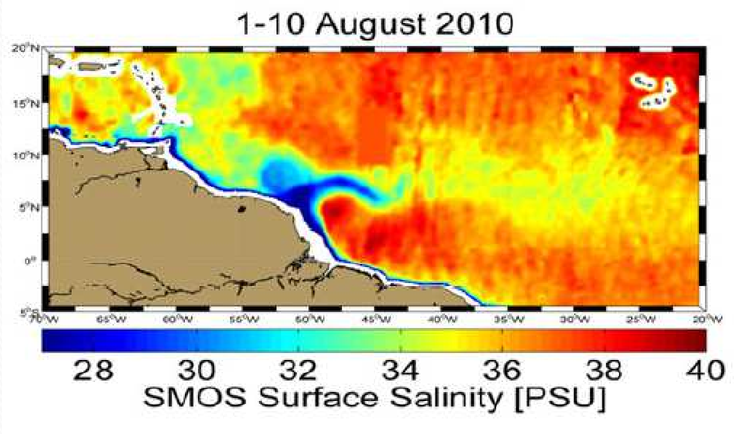

65% of the historical
TC that crossed the
Amazon Plume
evolved into cat 5 Hurricanes

A. Ffield (2007)

Fresh water wakes behind hurricanes

SSS wake ?

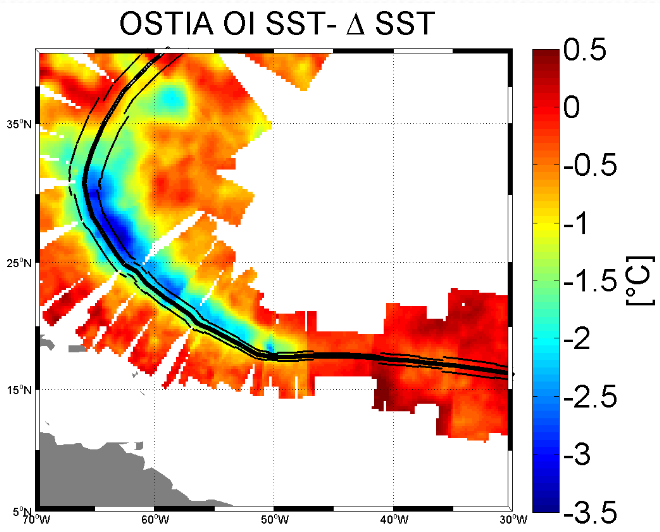

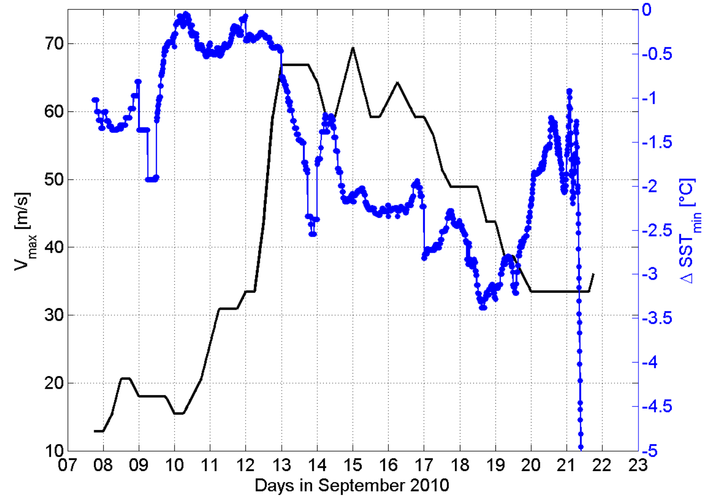

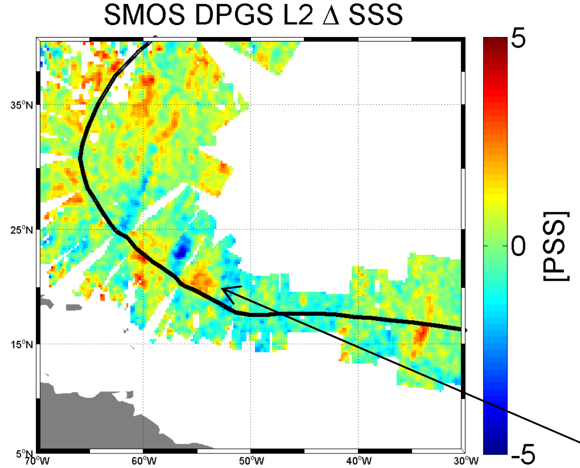

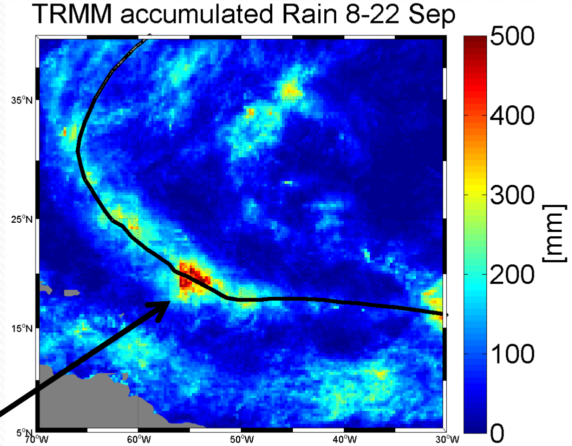

No clear signal